Understanding aerosol composition in a tropical inter-Andean valley impacted by agro-industrial and urban emissions

Lady Mateus-Fontecha[1], Angela Vargas-Burbano[1], Rodrigo Jimenez*[1], Nestor Y. Rojas[1], German Rueda-Saa [2], Dominik van Pinxteren[3], Manuela van Pinxteren[3], Khanneh Wadinga Fomba[3], Hartmut Herrmann[3]

[1] Universidad Nacional de Colombia – Bogota, Department of Chemical and Environmental Engineering, Air Quality Research Group, Bogota, DC 111321, Colombia

[2] Universidad Nacional de Colombia – Palmira, Department of Engineering and Management, Environmental Prospective, Research Group, Palmira, Valle del Cauca 763533, Colombia

[3] Leibniz Institute for Tropospheric Research (TROPOS), Atmospheric Chemistry Department (ACD), Permoserstrasse. 15, 04318, Leipzig, Germany.

Correspondence to: Rodrigo Jimenez (rjimenezp@unal.edu.co)

Abstract.

Agro-industrial areas are frequently affected by various sources of atmospheric pollutants that have a negative impact on public health and ecosystems. However, air quality in these areas is infrequently monitored because of their smaller ~~lower~~ population ~~density~~ compared to large cities, especially in developing countries. The Cauca River Valley (CRV) is an agro-industrial region in Southwest Colombia, where a large fraction of the area is devoted to sugarcane and derivative production. The CRV is also affected by road traffic and industrial emissions. This study aims to elucidate the chemical composition of particulate matter fine mode ($PM_{2.5}$) and to identify the main pollutant sources before source attribution. A sampling campaign was carried out at a representative site in the CRV region, where daily-averaged mass concentrations of $PM_{2.5}$ and the concentrations of water-soluble ions, trace metals, organic and elemental carbon, and various fractions of organic compounds (carbohydrates, n-alkanes, and polycyclic aromatic hydrocarbons – PAHs) were measured. The mean $PM_{2.5}$ was 14.4 ± 4.4 μg m^{-3}, and the most abundant constituent was organic material (53.0% ± 17.8%), followed by ammonium sulfate (16.1% ± 4.0%), and elemental carbon (7.0% ± 2.5%), which indicates secondary aerosol formation and incomplete combustion. Levoglucosan was present in all samples with a mean concentration of (113.8 ± 147.2 ng m^{-3}) revealing biomass burning as a persistent source. The diagnostic ratios applied to organic compounds revealed the influence of petrogenic and pyrogenic sources. ~~Principal component analysis identified the influence of traffic-generated road dust, secondary aerosol formation, gasoline and diesel~~

~~combustion vehicle exhaust, vegetative detritus, and resuspended agriculture soil. However, no single component was dominant nor explained the CRV $PM_{2.5}$ chemical species variance. Many components had equally important roles instead. Likewise, sugarcane pre-harvest burning (PHB), a frequent activity in CRV, was not identified as an independent component. This aerosol and trace gas source contributed to various components and was correlated to the formation of secondary aerosols.~~

Keywords: agro-industry; pre-harvest burning; $PM_{2.5}$; chemical speciation; principal component analysis; Northern South America

1. Introduction

Frequently, moderate to high population density, industrial presence, traffic, and other anthropogenic activities are linked with urban and suburban locations. Therefore, it is expected that the air quality and fine particulate matter (PM) will be impacted by these activities. In developing countries, suburban areas may be impacted by agricultural activities (Begam et al., 2016) (references) and are the least monitored despite the extensive use of high emission practices, including the intensive use of insecticides and pesticides and fire for land and crop management (Aneja et al., 2008, 2009). All these sources emit pollutants such as volatile organic compounds (VOC) that can form tropospheric ozone (Majra, 2011) and secondary organic aerosols (SOA) (Majra, 2011). $PM_{2.5}$ consists of solid and liquid particles with an aerodynamic diameter smaller than 2.5 µm, some of which contain black carbon (BC), and trace gases (including CO, CO2, SO2, NOx, NH3, VOC) that also generate O3 and SOA, all of which affect human health and climate (Yadav and Devi, 2019). Furthermore, agricultural operations are a significant source of nitrogen-containing trace gases (NO_2, NO, NH_3, N_2O) that are released from fertilizers, livestock waste, and farm machinery into the atmosphere (Sutton et al., 2011).

The Cauca River Valley (CRV) is an inter-Andean valley in Southwest Colombia with a flat area of 5287 km^2 (248-km long by 22-km mean width), a mean altitude of 985 m MSL (Figure 1) and is bounded by the Colombian Andes Western and Central Cordilleras and located at ~120 km from and meteorologically influenced by the Pacific Ocean. CRV encompasses the cities of Cali, Colombia's third-largest city with 2.2 million inhabitants (hab), Yumbo (129 khab), an important industrial hub, and Palmira (313 khab), which is surrounded by a multiplicity of agro-industrial activities in conjunction with other typical activities observed in urban and suburban areas.

The CRV hosts a highly efficient, resource-intensive sugarcane agro-industry with one of the greatest biomass yields and the highest sugar productivity in the world (~13 ton sugar/ha) (Asocaña, 2018, 2019). The operations of sugarcane farming and harvesting, as well as the transport of the biomass to the mill factories, are all part of the sugar mill industry. Besides, the industrial process includes the use of sugarcane bagasse to cogenerate energy in boilers. Other significant agro-industrial

activities present in the CRV include poultry and livestock production. The CRV is the third-largest national producer of poultry (351104 tons) and the first in egg production (4559 million units per year) (Min.Agricultura, 2020). In addition, the CRV produces 15.1% of national pork production (more than 1 million pigs) (Min.Agricultura, 2019) and 1.8% of national beef production (467,782 head) (Min.Agricultura, 2018). Likewise, as part of the typical urban and suburban areas, anthropogenic emissions derived from the densely populated are the mobile sources. The CRV has 1,951,638 vehicles that include the following vehicle types: passenger cars, motorcycles, buses, taxis, and off-road unregulated farming machinery. Besides, sugarcane agroindustry uses multi-car agricultural trailers towed by diesel-powered tractors, with enough annual activity to be considered an independent source, but with their activity tied to sugarcane harvesting. In general, all mobile activities in 2018 consumed 772 ML of gasoline and 590 ML of diesel fuel (SICOM, 2018). Furthermore, in terms of air traffic emissions, the local airport is a hub of the Colombian west handled 1.3 million flights in a typical year (Aerocivil, 2019). The other main economic line in CRV is the manufacturing industry, located mainly in the seven largest cities in the CRV: Cali, Tuluá, Cartago, Jamundí, Yumbo, Buga and Palmira.

For this research, we made a preliminary estimation of the aggregated PM_{10} emissions in CRV by putting together disparate source data, including from the stationary source emission inventories of CRV's six largest cities excluding Palmira (Cali, Tulua, Cartago, Jamundi, Yumbo and Buga), Cali's and other cities, mobile source emission inventories from Cali and other cities, and estimation of sugarcane PHB ~~(Cardozo-Valencia et al., 2019),~~ (Table S~~1~~). According to our preliminary estimates, the manufacturing industry, is the major PM_{10} emitter in CRV, with annual emissions of 10.5 kton PM_{10},. PM_{10} emissions from mobile sources (3.12 kton PM_{10} $year^{-1}$) and open-field sugarcane burning (1.3 kton PM_{10} $year^{-1}$) are a factor ~3 and ~8 smaller, respectively. Nonetheless, it is worth mentioning the following: 1) The available information was insufficient for estimating $PM_{2.5}$ emission estimation; 2) No emission data were available on Palmira, the city where our measurement site is located; 3) The stationary emission inventory of Yumbo, an industrial hub with the largest industrial activity, is outdated and very likely overestimated, particularly as a significant fraction of coal-fired boilers there have been converted to natural gas. The multiplicity, disparity, and uncertainty of sources are indicative of the complexity of the $PM_{2.5}$ source identification, quantification, and location tasks.

Studying the airborne PM chemical composition can be instrumental for the identification of pollutant sources, including agricultural burning, and the estimation of their contribution to the pollution burden. Most of the field measurement-based studies have been conducted in North America, Europe, and Asia (Karagulian et al., 2015). The number of studies in Latin America and the Caribbean (LAC) is smaller and have focused on the chemical composition of PM_{10} (Pereira et al., 2019; Vasconcellos et al., 2011), as well as the PM source apportionment in urban areas of Colombia (Ramírez et al., 2018; Vargas et al., 2012), Chile (Jorquera and Barraza, 2012, 2013; Villalobos et al., 2015), Costa Rica (Murillo et al., 2013) and Brazil (de Andrade et al., 2010). However, in relation to the agro-industrial and suburban areas, regions such as Indo-Gangetic plain

(Alvi et al., 2020), Sao Paulo in Brazil (Gonçalves et al., 2016; Urban et al., 2016), Ouagadougou in Burkina Faso (Boman et al., 2009), Anhui Province in China (Li et al., 2014) has documented $PM_{2.5}$ chemical composition and has identified some sources. Likewise, regions in South America with sugarcane agroindustry such as Mexico (Mugica-Alvarez et al., 2015; Mugica-Álvarez et al., 2016, 2018) and Brazil (de Andrade et al., 2010; De Assuncao et al., 2014; Lara et al., 2005; Pereira et al., 2017) also have reported the impact of this agro-industry on $PM_{2.5}$ at nearby population centers. However, studies about agroindustry areas are scarce in Colombia. In the CRV, only Romero et al., (2013) measured PAHs and metals in PM_{10}. Biomass burning and fossil fuel combustion were recognized as sources in all studies, and some identified industrial and fertilizer sources as well.

~~Due to their higher population and population density, air quality in urban areas has disproportionately received much more attention, from policymakers, governments, and researchers, than rural areas. Sometimes, this is grounded on the misconception that population sparsity implies lower exposure~~ (Majra, 2011)~~. Especially in developing countries, rural areas are the least monitored despite the widespread use of high emission practices, including the intensive use of insecticides/pesticides and fire for land and crop management~~ (Aneja et al., 2008, 2009)~~. Sprayed pesticides release volatile organic compounds (VOC) that can form tropospheric ozone~~ (Majra, 2011)~~ and secondary organic aerosols (SOA)~~ (Majra, 2011)~~, while whereas biomass burning (BB) emits fine particle particulate matter (PM) - consisting of solid and liquid particles with an aerodynamic diameter smaller than 2.5 μm, some of which contain black carbon (BC) , and trace gases (including CO, CO_2, SO_2, NO_x, NH_3, VOC) that also generate O_3 and SOA, all of which affect human health and climate~~ (Yadav and Devi, 2019)~~. Furthermore Additionally, agricultural activities are a significant source of nitrogen-containing traces gases (NO_2, NO, NH_3, N_2O) that are released into the atmosphere from fertilizers, livestock waste and farm machinery~~ (Sutton et al., 2011)~~.

~~The Cauca River Valley (CRV) is an inter-Andean valley in Southwest Colombia with a flat area of 5287 km^2 (248 km long by 22-km mean width), at a mean altitude of 985 m MSL (~~Figure 1~~), and is bounded by the Colombian Andes Western and Central Cordilleras, and located at ~120 km from and meteorologically influenced by the Pacific Ocean. CRV encompasses the cities of Cali, Colombia's third largest city with 2.2 million inhabitants (hab), Yumbo (129 khab), an important industrial hub, and Palmira (313 khab), which is the centroid of surrounded by extensive sugarcane plantations. The CRV hosts a highly efficient, resource-intensive sugarcane agro-industry, with one of the highest biomass yields and the highest sugar productivity in the World (~13 ton sugar/ha)~~ (Asocaña, 2018, 2019)~~. In 2019, the sugarcane agro-industry produced 3.7% of Colombia's agricultural gross domestic product (GDP) and 2.2% of its industrial GDP (0.6% of the total GDP)~~ (Asocaña, 2019)~~. In 2018 the sugarcane harvest was 195,346 ha, with 25% belonging to 15 sugar mills and 75% to private owners~~ (Asocaña, 2019)~~. The production rate was 119.61 sugarcane ton/ha in 2018 and the average size of each crop was 63 ha. Sugarcane is used to produce granulated sugar and ethanol~~ (Asocaña, 2019)~~. A fraction of sugarcane is harvested using mechanical methods (45%) and the rest is cutter manually~~ (Asocaña, 2020)~~. In the manual method, the crops are burned for some minutes to facilitate manual cane~~

cutting. Manual harvesting provides low-skilled employment to the people of the region. About 69,272 ha (~8.3 Mt) of sugarcane were burnt in 2018, thus contributing to the emissions of PM and gases (Cardozo-Valencia et al., 2019). In addition, 6.1 Mt of sugarcane bagasse are used to generate electricity (1,657 GWh) (Asocaña, 2020), emitting $PM_{2.5}$, Volatile Organic Compounds (VOCs), Carbonyls, PAHs, and other combustion pollutants (Hall et al., 2012). The transport of all sugarcane produces to mill industries is always carried out in multi-car agricultural trailers towed by diesel-powered tractors. The tractor fleet is old and numerous, with enough annual activity to be considered an independent source with its own emission chemical profile, like other diesel sources, but with its activity tied to sugarcane harvesting. CRV is an agro-industrial area with relevant poultry and livestock production being the third-largest national production of poultry (351104 tons) and eggs (4559 million units per year) (Min.Agricultura, 2020). In addition, CRV produces 15.1% of national pork production (more than 1 million pigs) (Min.Agricultura, 2019), and 1.8% of national beef production (467,782 head) (Min.Agricultura, 2018). The mobile sources inventory highlight the role of fossil fuel emissions in the CRV, with 1,951,638 vehicles that include vehicles type: passenger cars, motorcycles, buses, taxis, and off-road machinery, consuming 772 ML of gasoline and 590ML of diesel fuel (SICOM, 2018). In terms of air traffic emissions, the local airport is a hub of Colombian west handled 1.3 million flights in a typical year (Aerocivil, 2019).

Agricultural burning is worldwide used as an agriculture practice for rapidly and inexpensively clearing the land, and for facilitating tillage and harvesting, so these can proceed unimpeded by external factors. This practice not only results in serious environmental local issues, like the increase of respiratory diseases for the population that is directly exposed, but also it is one of the main contributors to global atmospheric pollution (Abdurrahman et al., 2020). Biomass burning is common in tropical areas of Africa (Dajuma et al., 2020; Li et al., 2020; Mkoma et al., 2013; Van Wees and Van Der Werf, 2019), South America (Lara et al., 2005; Mugica-Alvarez et al., 2015; Pereira et al., 2017; Romero et al., 2013), Asia (Janta et al., 2020; Pongpiachan et al., 2017), and Australia (He et al., 2016). Although widespread, open agricultural fires are typically shorter and less intense than forest fires, which make difficult their satellite detection and quantification (Pan et al., 2020). This has further hindered their observation and analysis. The pre-harvest burning (PHB) of wheat, corn, rice residues, and sugarcane has been documented in Mexico (Mugica-Alvarez et al., 2015), Colombia, (Romero et al., 2013), Brazil (Lara et al., 2005; Vasconcellos et al., 2007) and Thailand (Janta et al., 2020). Sugarcane is a crop of global importance (26.8 million hectares in 2019) (FAO, 2020). About 80% of sugar and almost half of bioethanol worldwide are produced from sugarcane cultivated in more than 90 countries, most of them in the Global South but also in some developed economies, including Australia and USA (FAO, 2020).

Sugarcane PHB is still a very common practice worldwide. As other open-field BB practices, sugarcane burning emits aerosols of high toxicity, such as PAH, which produce inflammation of epithelium and vascular endothelial adhesion molecules (Chen et al., 2017; Johnston et al., 2019). BB can also intensify the formation of secondary inorganic particles due to the interaction

of smoke plumes with pollutants emitted in urban and industrial areas (Wang et al., 2015). In addition, BB emits BC, which is considered a short-lived climate pollutant (Chen et al., 2017).

Studying the airborne particulate matter PM chemical composition can be instrumental for the identification of pollutant sources, including agricultural burning, and the estimation of their contribution to the pollution burden. Most of the field measurement based studies have been conducted in North America, Europe, and Asia (Karagulian et al., 2015). The number of studies in Latin America and the Caribbean (LAC) is smaller and have focused on the chemical composition of PM_{10} (Pereira et al., 2019; Vasconcellos et al., 2011), as well as the and the PM source apportionment in urban areas of Colombia (Ramírez et al., 2018; Vargas et al., 2012), Chile (Jorquera and Barraza, 2012, 2013; Villalobos et al., 2015), Costa Rica (Murillo et al., 2013) and Brazil (de Andrade et al., 2010). Previous PM chemical characterization studies in agricultural areas with pre- and post-harvest sugarcane burning have been conducted in Brazil (de Andrade et al., 2010; De Assuncao et al., 2014; Lara et al., 2005; Dos Santos et al., 2002; Souza et al., 2014; Urban et al., 2012, 2016), and México (Mugica-Alvarez et al., 2015; Mugica-Álvarez et al., 2016). Other studies have investigated the emissions from sugarcane burning in combustion chambers for PM_{10}, $PM_{2.5}$, Elemental Carbon (EC), Organic Carbon (OC) and PAHs (Hall et al., 2012; Jenkins et al., 1992; Mugica-Álvarez et al., 2018).

Although communities, environmental authorities, and the scientific community have long acknowledged the public health, environmental, and climate implications of open sugarcane burning, research in Colombia is limited (Dávalos, 2007; IDEAM, 2018; Romero et al., 2013). Research in Colombia is scarce (Romero et al., 2013), even though communities, environmental authorities, and the scientific community have long recognized the public health, environmental, and climate impacts of open sugarcane burning, especially in the Cauca River Valley (CRV) (Dávalos, 2007; IDEAM, 2018).

CRV is an inter-Andean valley in Southwest Colombia with a flat area of 5287 km^2 (248 km long by 22 km mean width), at a mean altitude of 985 m MSL (Figure 1), bounded by the Colombian Andes Western and Central Cordilleras, and located at ~120 km from and meteorologically influenced by the Pacific Ocean. CRV encompasses the cities of Cali, Colombia's third-largest city with 2.2 million inhabitants (hab), Yumbo (129 khab), an important industrial hub, and Palmira (313 khab), which is the centroid of surrounded by extensive sugarcane plantations. CRV hosts a highly efficient, resource-intensive sugarcane agro-industry, with one of the highest biomass yields and the highest sugar productivity in the World (~13 ton sugar/ha) (Asocaña, 2018, 2019). The sugarcane agro-industry produced 3.7% of Colombia's agricultural gross domestic product (GDP) and 2.2% of its industrial GDP (0.6% of the total GDP) in 2019 (Asocaña, 2019). In 2018 the sugarcane harvest was 195,346 ha, of which 25% belong to 15 sugar mills and 75% to private owners (Asocaña, 2019). The production rate was 119.61 sugarcane ton/ha in 2018 and the average size of each crop is 63 ha, to produce powdered sugar and ethanol used as biofuel (Asocaña, 2019). A fraction (45%) of sugarcane is harvested using a mechanical method and the other fraction (55%) with a manual labor method (Asocaña, 2020). In the manual method, the crops are burned for some minutes to facilitate the process

~~of cane cutters and this manual harvest also is used as a socioeconomic tool to provide low skilled employment to the population of the region. About 69,272 ha (~8.3 Mt) of sugarcane were burnt in 2018, thus contributing to the emissions of PM and gases (Cardozo-Valencia et al., 2019). Since 6.1 Mt of sugarcane bagasse are used to generate electricity (1,657 GWh) (Asocaña, 2020), this adds additional emissions of $PM_{2.5}$ and organic components such as Volatile Organic Carbons (VOCs), Carbonyls, and PAHs (Hall et al., 2012). Additionally, either pre-harvest burned or not, harvested sugarcane is transported to mills in multi-car trailers towed by diesel powered crawlers. The crawler fleet is aged and numerous enough, and with sufficient annual activity, to potentially constitute an independent source with its own emission chemical profile, similar to other diesel sources, but with its activity tied to sugarcane harvesting.~~

This research aimed to characterize the chemical composition of $PM_{2.5}$ at a representative location in the CRV, including EC, primary and secondary ~~organic carbon (~~OC~~)~~, ions, trace metals, and specific molecular markers, such as ~~including~~ ~~polycyclic aromatic hydrocarbons (~~PAH~~)~~, n-alkanes, and carbohydrates, as well as the ~~and to understand the~~ relationships between ~~among~~ these components and ~~with~~ emission sources. Diagnostic ratios ~~and principal component analysis~~ were used to identify the most important $PM_{2.5}$ components and as a tool for preliminary pollutant source attribution, including primary and secondary aerosols generated by or associated with sugarcane ~~pre-harvest burning (~~PHB~~)~~. We believe that in the CRV case, this analysis is needed prior to source apportionment with receptor models for three reasons: 1) This is the first comprehensive investigation of PM composition in the CRV (prior studies included two types of components at most); 2) There are no suitable chemical profiles for some pollutant sources, particularly sugarcane PHB; 3) Our measurements dataset is just barely large enough for profile-free receptor modeling (positive matrix factorization). Our results are particularly relevant for urban communities and atmospheres impacted by large-scale intensive agriculture and industrial emissions, particularly in developing countries, especially in Latin America where PM composition information is still scarce ~~sparse~~ (Liang et al., 2016).

2. Methods

2.1. Description of the sampling site

The sampling site was located on the rooftop of an 8-story administrative building at the Palmira Campus of Universidad Nacional de Colombia (3º30'44.26" N; 76º18'27.40" W, 1065 m altitude), about 27 m above the ground. The campus is located on the western outskirts ~~at the west edge~~ of Palmira's urban area ~~(311 khab)~~ and is surrounded by short buildings on the east, and extensive sugarcane plantations, several sugar mills, and other industries elsewhere. Palmira is located at ~27 km northeast of Cali ~~(2.2 Mhab)~~ and ~22 km southeast of Yumbo ~~(129 khab)~~, an important industrial hub. The Pacific Ocean coastline stretches ~~is located~~ at ~120 km across the Western Cordillera, as shown in Figure 1, and operates one of the busiest international trade seaports in the country~~. On the Pacific Ocean coast is one most important international trade seaports in Colombia~~. Most

of the freight is transported by diesel-powered trucks. Road traffic is also substantial within the CRV, with Bogota and along the Pan-American highway that connects Colombia with other South American countries.

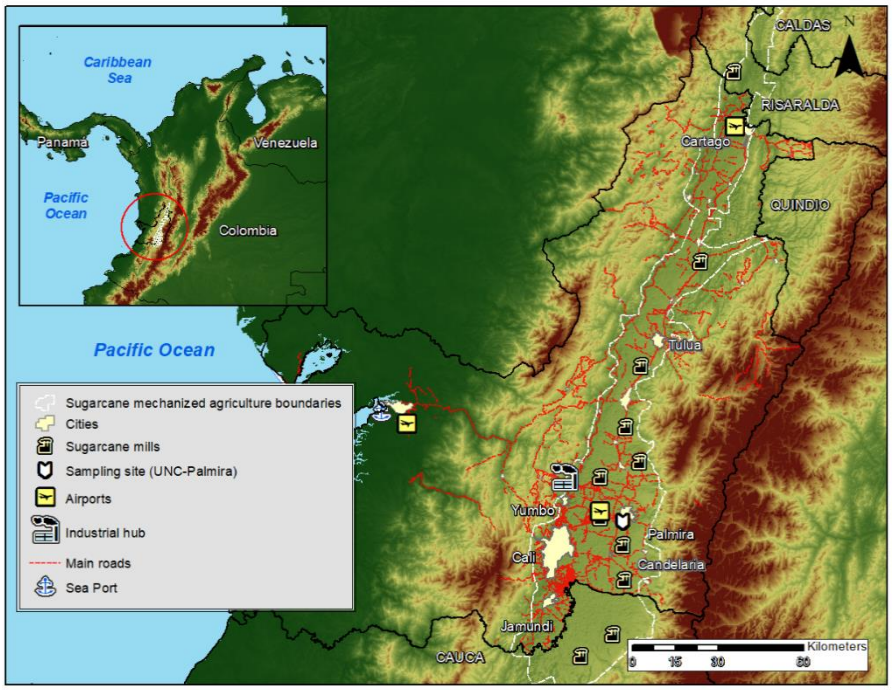

Figure 1. Map of the Cauca River Valley (CRV). The inset shows the location of the CRV in Colombia and in Northern South America. The map shows the main cities in the CRV, including Palmira (312 thousand inhabitants), our measurement site; ~~and~~ Cali, the most important city in the southwest of Colombia ~~with 2.2 million inhabitants~~; Yumbo, an industrial hub, and the main highways. Sugar mills, which produce sugar, bio-ethanol, and electric power are also shown. The dashed-line defined area is the CRV's flattest (slope < 5%) bottomland, where mechanized, intensive sugarcane agriculture takes place. Significant diesel combustion emissions occur along the Buenaventura highway because it is one of the busiest ports in Colombia on the Pacific Ocean. ~~Buenaventura on the Pacific Ocean is one of the busiest ports in Colombia, thus significant diesel combustion emissions occur along the Buenaventura highway.~~

The Andes Cordillera splits into three south-to-north diverging mountain ranges (Western, Central, and Eastern Cordilleras) near the Colombia-Ecuador border. ~~The CRV is an inter-Andean valley at ~985 m altitude located ~120 km from the Pacific Ocean, bounded by the Central and Western Cordilleras~~ (see Figure 1). The Western Cordillera separates the CRV from the Colombian Pacific Ocean watershed, the rainiest region on Earth (Hernández and Mesa, 2020) The elevated precipitation in this basin (Mesa and Rojo, 2020). is due to the presence of a Walker cell convergence zone at the surface, persistent under

neutral and La Niña conditions. This synoptic feature is one of the most important determinants of atmospheric circulation in Colombia, with prevailing east-to-west winds in the lower troposphere along with upper troposphere return winds (Mesa and Rojo, 2020). The Andean Cordilleras are nevertheless effective barriers to the Walker circulation near the CRV surface (Lopez and Howell, 1967; Mesa S. and Rojo H., 2020) ~~(Lopez and Howell, 1967)~~. The elevated humidity in the Pacific Ocean watershed and the closeness of the two Andes branches drive a zonal regional circulation pattern, consisting ~~in~~ of west-to-east anabatic winds over the Pacific slope of the Western Cordillera during the daytime followed by rapid katabatic winds in the late afternoon (Lopez and Howell, 1967). These winds rapidly ventilate the CRV during the late afternoon – early evening period on an almost regular basis. The CRV is wide (~22 km) and long (~248 km) enough to develop a valley-mountain wind circulation pattern during the daytime. Winds are very mild during this time period and expected to be highly dispersive, i.e. with high turbulence intensities (Ortiz et al., 2019). The arrival of the katabatic "tide" in the ~~at~~ late afternoon wipes the valley-mountain wind pattern out (Lopez and Howell, 1967).

2.2. Sampling protocols

The sampling campaign was conducted between July 25th and September 19th, 2018. $PM_{2.5}$ aerosol particles (aerodynamic diameter < 2.5 μm) were collected on Teflon and quartz fiber filters simultaneously for 23 h (from 12:00 local time – LT – to the ~~following~~ next day at 11:00 LT), using 2 in-tandem low-volume samplers (ChemComb speciation samplers, R&P). Each sampler used an independent pump set at a flow rate of 14 L min^{-1}. For both types of filters, three lab blank filters without exposure were analyzed. Quartz filters were pre-baked at 600 °C for 8 h before sampling to eliminate contaminant trace hydrocarbons. In total, 45 samples were collected. Prior to and after exposure, the filters were conditioned at constant humidity (36±1.5% relative humidity) and temperature (24 ± 1.2 ºC) for 24 h before being weighing on a microbalance (Sartorius, Mettler Toledo) with a 199.99 g capacity and 10 μg resolution. $PM_{2.5}$-loaded filters were saved at Petri boxes previously prepared to avoid cross-contamination of organic species. The filters were subsequently were stored at –20°C until analysis to reduce the volatilization of species such as ammonium nitrate and semi-volatile organic compounds. Blank quartz filters were pre-baked and stored following an identical procedure to exposed filters to collect samples. Blank Teflon filters were treated under the same conditions of storage, transport, and analysis as $PM_{2.5}$-loaded filters.

By differential weighing, mass concentrations were determined from the Teflon filters. It's worth mentioning that during the sampling period, 1888 sugarcane ~~pre-harvest burning~~ PHB episodes ~~events~~ occurred. ~~took place during the sampling period.~~ This register was made by the regional environmental agency (CVC, as per its acronym in Spanish), using information from sugar mills about PHB events. The vast majority of these events were intentional, controlled, size-limited (~6 ha median area), and brief ~~short~~ (~25-minute median duration) (Fig S1).

2.3. Analytical methods

The quartz-fiber filter samples were analyzed for ions, metals, elemental and organic carbon, and speciation of the carbonaceous fraction. The Teflon-membrane filter samples were analyzed for metals.

Two circular pieces ~~of quartz filter~~ with an ~~of~~ 8 mm diameter (100.5 mm^2) were punched from ~~the~~ each quartz and Teflon filter, following the method described by Wadinga Fomba et al., (2020), and extracted using 1 mL of ultrapure water (18 MΩ) in a shaker at 400 rpm for 120 min. The extracts were filtered through 0.45 µm syringe filters (Acrodisc Pall). An aliquot of the solution was analyzed for inorganic (K^+, Na^+, NH_4^+, Mg^{2+}, Ca^{2+}, Cl^-, NO_3^-, SO_4^{2-}, NO_2^-, PO_4^{3-}, Br^-, F^-) and some organic ions ($C_2O_4^{2-}$, $CH_3O_3S^-$, and CHO_2^-) by ion chromatography (IC690 Metrohm; ICS3000, Dionex). Another aliquot was analyzed for carbohydrates, including levoglucosan, mannosan, and galactosan, as described by Iinuma et al. (2009a). Organic and elemental carbon were determined from 90.0 mm^2 filter pieces following the EUSAAR 2 protocol (Cavalli et al., 2010), with a thermal-optical method using a Sunset Laboratory dual carbonaceous analyzer.

Seventeen metals, including K, Ca, Ti, V, Cr, Mn, Fe, Ni, Cu, As, Se, Sr, Ba, Pb, Sn, Sb, and Cu, were analyzed from Teflon (22 samples) and quartz (23 samples) filters by total reflection X-Ray Fluorescence Spectroscopy – TXRF (TXRF, PICOFOX S2, Bruker). Si was not determined as this element is ~~makes~~ part of the quartz filter substrate. Metals were analyzed from three 8-mm circular pieces punched ~~of~~ from Teflon filters ~~from the 45 filters~~, which were digested ~~into~~ ~~after their digestion with~~ a nitric and chloride acid solution for 180 min ~~to~~ at 180 °C. After this, 20-µl aliquots of the digested solution were placed on the surface of polished TXRF quartz substrates along with 10 µl of Ga solution, which served as an internal standard. This solution was left to evaporate at 100°C. The samples were measured at two angles with a difference of 90° between them to ensure complete excitation of metals. More details on the analytical technique can be found in Fomba et al. (2013).

Alkanes and PAHs were determined from two circular ~~pieces of~~ filter punches (6 mm diameter, 56.5 mm^2), using a Curie-point pyrolyzer (JPS-350, JAI) coupled to a GC-MS system (6890 N GC, 5973inert MSD, Agilent Technologies). The chemical identification and quantification of the C_{20} to C_{34} n-alkanes, as well as ~~along with~~ the following organic species were performed using the following external standards (Campro, Germany): pristane, phytane, fluorene (FLE), phenanthrene (PHEN), anthracene (ANT), fluoranthene (FLT), pyrene (PYR), retene (RET), benzo(b)naphtho(1,2-d)thiophene (BNT(2,1)), cyclopenta(c,d)pyrene (CPY), benz(a)anthracene (BaA), chrysene(+Triphenylene) (CHRY), 2,2-binaphtyl (BNT(2,2)), benzo(b)fluoranthene (BbF), benzo(k)fluoranthene (BkF), benzo(e)pyrene (BeP), benzo(a)pyrene (BaP), indeno (1,2,3-c,d)pyrene (IcdP), dibenz(a,h)anthracene (DahA), and benzo(g,h,i)perylene (BghiP), coronene (COR), 9H-Fluoreneone (FLO(9H)), 9,10-Anthracenedione (ANT (9,10)) and 1,2-Benzanthraquinone (BAQ (1,2)). Four deuterated PAHs, (acenaphthene-d10, phenanthrene-d10, chrysene-d12, and perylene-d12), and two deuterated alkanes (tetracosane-d50 and

tetratriacontane-d70) were used as internal standards, following the analytical method described by (Neusüss et al., 2000). For each analyzed compound, the sample concentration was calculated by subtracting the average concentration of three blank filters from the measured concentration.

~~2.4.~~ Diagnostic ratios and mass closure ~~Mass closure and diagnostic ratios~~

~~$PM_{2.5}$~~ The main $PM_{2.5}$ components were estimated from the concentrations of EC, OC, water-soluble ions (NO_3^-, SO_4^{2-}, NH_4^+, and Na^+), and tracer metal concentrations (Ca, Ti, Fe, Ni, Cu, Zn, As, Se, Sb, Ba, and Pb)~~. The main components considered were~~ as follows: organic material (OM), EC, ammonium sulfate ($(NH_4)_2SO_4$), ammonium nitrate (NH_4NO_3), crustal material (dust), other trace elements oxides (TEOs), and particle-bounded water (PBW)~~, and sea salt (SS), reckoned as sodium chloride~~. $PM_{2.5}$ closure is described by Eq 1 (Dabek-Zlotorzynska et al., 2011). ~~Except for EC, these components were not directly determined by chemical analysis, but calculated from concentrations of the chemical species measured.~~ We used the Interagency Monitoring of Protected Visual Environment (IMPROVE) equations (Chow et al., 2015) to quantify the concentrations of main compounds (Table 1). ~~Equations (Chow et al., 2015). See Table 1. Also, this reconstruction which are shown in Table 1. Also, this reconstruction was instrumental towardsin the identification of the main fine airborne particle sources.~~ The aerosol particle bounded water content was estimated from the measured ionic composition, relative humidity, and temperature, following the aerosol inorganic model (AIM) described by (Clegg and Peter Brimblecombe, 1998), which is available for running online at http://www.aim.env.uea.ac.uk/aim/model2/model2a.php. ~~AIM describes the thermodynamic equilibrium of the system~~ The thermodynamic equilibrium of the system H^+- NH_4^+ - SO_4^{2-} - NO_3^-- H_2O is described by AIM.

$$PM_{2.5}(mass\ closure\ estimated) = OM_{pri} + OM_{sec} + EC + NH_4SO_4 + NH_4NO_3 + Dust + TEO + SS + PBW \quad \text{Eq (1)}$$

Table 1. Equations used to estimate the main components of $PM_{2.5}$

Component	Equation	Reference
OM_{prim}	$= f_1\ OC_{prim}$	(Chow et al., 2015) (Turpin and Lim, 2001)
OM_{sec}	$= f_2\ OC_{sec}$	(El-Zanan et al., 2005)
$(NH_4)_2SO_4$	$= 1.3754(SO_4^{2-})_{nss}$ Where $(SO_4^{2-})_{nss} = (SO_4^{2-}) - 0.252Na^+$	(Chow et al., 2015)
$(NH_4)NO_3$	$= 1.29(NO_3^-)$	(Chow et al., 2015)
SS	$= 2.54(Na^+)$	(Chow et al., 2015) (Snider et al., 2016)
Dust	$= 1.63Ca + 1.94Ti + 2.42Fe$ (Assuming CaO, Fe_2O_3, FeO (in equal amounts) and TiO_2)	(Chow et al., 2015)
PBW	$= k\ (SO_4^{2-} + NH_4^+)$	(Clegg and Peter Brimblecombe, 1998)
TEO	$= 1.47[V] + 1.27[Ni] + 1.25[Cu] + 1.24[Zn] + 1.32[As] + 1.2[Se] + 1.07[Ag] + 1.14[Cd] + 1.2[Sb] + 1.12[Ba] + 1.23[Ce] + 1.08[Pb]$	(Snider et al., 2016)

f_1 = 1.6. This factor was estimated considering the predominant sources.
f_2 = 2.1. This factor was estimated by subtracting the non-carbon component of $PM_{2.5}$ from the measured mass.
k = 0.32 was calculated using the Aerosol Inorganic Model.

The EC tracer method was applied to estimate primary (OC_{prim}) and secondary (OC_{sec}) organic carbon (Lee et al., 2010). This method utilizes EC as a tracer for primary OC, which implies that OC_{prim} from non-combustion sources ~~OC_{prim}~~ is deemed negligible. Primary and secondary OC can be estimated by ~~upon~~ defining a suitable primary OC to EC ratio ($[OC/EC]_{prim}$). See Eq (2) and Eq (3). We estimated the $[OC/EC]_{prim}$ ratio as the slope of a Deming linear fit between EC and OC measurements. The term b corresponds to the linear fit intercept, which can be interpreted as the emitted OC_{prim} that is not associated with EC emissions. This method is limited by the following assumptions: 1) $[OC/EC]_{prim}$ is deemed constant, despite the reality that it may change throughout the day depending on factors such as ~~while in fact this ratio might change during the day according e.g. to the~~ wind direction and the location of the dominant emission sources. Our 23-h sampling is expected to smooth this variability source out; 2) It neglects OC_{prim} from non-combustion sources; and 3) It assumes that OC_{prim} is nonvolatile and nonreactive. Departure from these assumptions implies that the estimation of OC_{prim} and OC_{sec} might be biased, likely underestimating OC_{sec}.

$$OC_{prim} = [OC/EC]_{min} * EC + b \qquad \text{Eq (2)}$$

$$OC_{sec} = OC - OC_{prim} \qquad \text{Eq (3)}$$

OCprim was also estimated by using an organic tracer method. A simple linear model was applied to find the proportion of OC_{prim} from three sources that are significant in the CRV, namely fossil fuel combustion (OC_{FF}), biomass burning (OC_{BB}), and vegetable detritus (OC_{det}). OC_{FF}, OC_{BB} and OC_{det} was quantified using a linear model from the following tracers: BghiP and IcdP for fossil fuel; levoglucosan for biomass burning; and the sum of the highest molecular weight alkanes (C_{27} – C_{33}) for vegetable detritus.

According to ~~As per~~ Table 1, OM was estimated from OC using conversion factors f_1 and f_2 (Chow et al., 2015), which are dependent on the OM oxidation level and the secondary organic aerosol formation and aging during transportation. ~~Aiken et al., (2008) compared OM/OC ratios for several Primary Organic Aerosols (POA) and Secondary Organic Aerosol (SOA) sources, based on O/C ratios measured by elemental analysis, establishing the following trend for its ratios: POA < BBOA < OOA (as characteristics of aged and fresh SOA). For fossil fuel combustion emission input a value of traffic. Some of the main sources of POA that could be present in CRV are derived from industrial emissions and biomass burning emissions. Aiken et al., (2008) used a trend for OM/OC ratios, values between 1.56 – 1.70 for BBOA, while XX suggest ~ 2.0. Main sources of SOA~~

Turpin and Lim (2001a) recommended an OM/OC ratio of 1.6 ± 0.2 for urban aerosols, and 2.1 ± 0.2 for non-urban aerosols, values comparable with those found by Aiken et al. (2008), ~~which related OM/OC through factor~~ of 1.71 (1.41 – 2.15), where lower values (1.6 – 1.8) are attributed to ground measurements in the morning ~~time~~, and higher values (1.8 – 1.9) ~~corresponding~~ to aircraft sample measurements. ~~Biomass burning~~ BB aerosols can have ~~an~~ even higher *f* values (2.2-2.6), due to the presence of organic components with higher molecular weights, e.g., levoglucosan. However, Andreae (2019) recommends a factor of 1.6 for fresh BB aerosol, which is consistent with Hodshire et al (2019). We believe that traffic and biomass burning are the dominant OC_{prim} sources at ~~out~~ our site. Therefore, we used ~~an~~ f_1 = 1.6 to estimate OM_{pri}. We used a factor of 2.1 to estimate OM_{sec} from the OC_{sec} fraction. This factor was chosen based on recommended ratios of 2.1±0.2 for aged ~~or non-urban~~ aerosols. ~~and ii) the molecular weight to carbon weight ratio for levoglucosan of 2.2. Levoglucosan is taken as component of reference due to its abundance in samples collected where the biomass burning happens often and as shown in section 3.6, levoglucosan was a tracer present in whole samples collected in this study~~ (Schauer, 1998)~~.~~

Concentration ratios among distinct species were used to chemically characterize and infer the main sources of fine particle matter at Palmira. As a preliminary proxy for $PM_{2.5}$ acidity, the cation/anion equivalent ratio and the $[NH_4^+]/[SO_4^{2-}]$ molar ratio were used. The first one is based on electroneutrality and assumes that H^+ balances the excess of anions in the solution considered, and the second one ratio is an indicator of acidity attributable to those two ions, which are usually the most abundant cation and anion contained in the $PM_{2.5}$. The cation equivalent to anion equivalent ratio was calculated using Eq (4) and Eq (5) for each term.

However, these approaches to inferring the $PM_{2.5}$ acidity can result in challenging interpretations, incomplete and incorrect results due to an indirect connection to the system's acidity (Pye et al., 2020). Therefore, the E-AIM (Extended Aerosol Inorganics Model) was used to determine the equilibrium state of a system containing water and the following ions: SO_4^{2-}, NH_4^+, NO_3^-, Na^+ and Cl-, with an atmosphere of known temperature and relative humidity, without information on gas-phase concentrations (NH_3, HNO_3 and SO_2), which were not available in this study. The H^+ mole fraction concentration from E-AIM IV (Friese and Ebel, 2010), was used to calculate pH following Eq (6). E-AIM requires that the input data for ionic composition be balanced on an equivalent basis, which means that the sums of the charges on the cations and anions considered in the system do balance, accordingly $[SO_4^{2-}] + [NO_3^-] + [Cl^-] = [NH_4^+] + [Na^+]$. The disadvantage of this approach is that it does not allow for the partitioning of trace gases into the vapor phase. The model is available to run on the following website: http://www.aim.env.uea.ac.uk/aim/model4/model4a.php (last access: 22 January 2022).

$$AE = \frac{[SO_4^{2-}]}{48} + \frac{[NO_3^-]}{62} + \frac{[C_2O_4{}^{2-}]}{44} + \frac{[Cl^-]}{35} + \frac{[PO_4^{3-}]}{31.3} + \frac{[NO_2^-]}{46} + \frac{[Br^-]}{79.9} + \frac{[F^-]}{18.9} + \frac{[CH_3O_3S^-]}{95} + \frac{[CHO_2^-]}{45} \quad \text{Eq (4)}$$

$$CE = \frac{[Na^+]}{23} + \frac{[K^+]}{39} + \frac{[NH_4^+]}{18} + \frac{[Mg^{2+}]}{12} + \frac{[Ca^{2+}]}{20} \quad \text{Eq (5)}$$

$$pH_x = -log_{10}(a_{H^+}^x) \quad \text{Eq (6)}$$

Parent PAH ratios are widely used to identify combustion-derived PAH (Khedidji et al., 2020; Szabó et al., 2015; Tobiszewski and Namieśnik, 2012), although some of them are photochemically degraded in the atmosphere (Yunker et al., 2002). Additionally, n-alkanes are employed ~~used~~ as markers of fossil fuel or vegetation contributions to $PM_{2.5}$. ~~The parameters used to elucidate the n-alkane origin were~~ Carbon number maximum concentration (C_{max}), carbon preference index (CPI)m, and wax n-alkanes percentage (WNA%) were the criteria utilized to determine the n-alkane origin. Table 2 summarizes the diagnostic ratio equations and the expected dominating source ~~according to~~ based on the ratio value.

Table 2. Diagnostic ratios of organic compounds used to infer the sources of $PM_{2.5}$ in this study.

Diagnostic ratios	Equation	Value	Source	References
BeP/(BeP+BaP)		~0.5 < 0.5	Fresh particles Photolysis	(Tobiszewski and Namieśnik, 2012)
IcdP/(IcdP+BghiP)		<0.2 0.2 - 0.5 >0.5	Petrogenic Petroleum combustion Grass, wood and coal combustion	(Yunker et al., 2002) (Tobiszewski and Namieśnik, 2012)
BaP/BghiP		<0.6 >0.6	Non-traffic emissions Traffic emissions	(Tobiszewski and Namieśnik, 2012) (Szabó et al., 2015)
IcdP/BghiP		>1.25 <0.4	Brown coal* Gasoline	(Ravindra et al., 2008)
LMW/(MMW+HMW)		<1 >1	Pyrogenic Petrogenic	(Tobiszewski and Namieśnik, 2012)
C_{max}		< C_{25} $C_{27} - C_{34}$	Anthropogenic Vegetative detritus	(Lin et al., 2010)
CPI	$CPI = 0.5 * \left[\frac{\sum_{19}^{33} C_i}{\sum_{20}^{32} C_k} + \frac{\sum_{19}^{33} C_i}{\sum_{22}^{34} C_k}\right]$	CPI ~1 CPI > 1	Fossil carbon Biogenic	(Marzi et al., 1993) (Kang et al., 2018)
WNA%	$\sum WNA_{C_n} = [C_n] - \left[\frac{(C_{n+1}) + (C_{n-1})}{2}\right]$ $WNA\% = \frac{\sum WNA_{C_n}}{\sum Total\ n-alkanes}$ $PNA\% = 100 - WNA\%$	WNA ~ 100 PNA ~ 100	Biogenic Anthropogenic	(Lyu et al., 2019)

*Used for residential heating and industrial operation.

As all ~~the~~ measured variables were subject to analytical uncertainty and temporal variability, linear fitting parameters were obtained from Deming regressions as recommended for atmospheric measurements (Wu and Zhen Yu, 2018). The Spearman coefficient was selected instead of Pearson's as an indicator of statistical correlation between chemical components ~~instead of Pearson's~~ to reduce the effect of outliers. Derived ratios and other parameters were considered statistically significant when p-values < 0.05. The statistical analysis was conducted ~~made~~ using R version 4.0.2, 24 including the packages corrr (0.4.2), mcr (1.2.1), cluster (2.1.0), tidyverse (1.3.0), ggplot (3.3.2), psych (2.0.9) and openair (2.7-4).

~~2.5. Principal component analysis (PCA)~~

~~There is very little information in the literature on the composition of several of the aerosol emission sources deemed important in CRV. This is particularly true for sugarcane PHB and sugarcane bagasse combustion. Because of this, instead of directly jumping into a source attribution effort, using receptor modeling methods, we deemed it more important at this stage of our research to apply multivariate statistical techniques to unravel correlations among the various aerosol components and to~~

potentially identify various aerosol sources. For this, we applied principal component analysis (PCA). We consider this useful in our case, even if PCA is nowadays considered an outdated technique for source attribution in regions with reasonably characterized sources (Hopke, 2016). The species Br^-, $C_{19}H_{40}$, COR, and manosan were excluded from these analyses because more than 80% of their concentrations were below the detection limit (BDL). Data were organized into a matrix of 45 $PM_{2.5}$ samples (rows) times 73 chemical species (columns). BDL "missing" values were replaced by corresponding species detection limit. To reduce skewness and order of magnitude effects, the concentration dataset was log10 transformed, mean centered, and scaled to unit variance. Principal components were derived from the correlation matrix. We applied varimax rotation PCA as rotated components have easier to interpret loadings. Principal components (PC) were selected to explain at least 60% of the total variance. Calculations were made with the Psych (2.0.9) R package.

3. Results and discussions

3.1. Meteorology

The Andes Cordillera splits into three south to north diverging mountain ranges (Western, Central, and Eastern Cordilleras) near the Colombia Ecuador border. The CRV is an inter Andean valley at ~985 m altitude located ~120 km from the Pacific Ocean, bounded by the Central and Western Cordilleras (see Figure 1). The Western Cordillera separates CRV from the Colombian Pacific Ocean watershed, the rainiest region on Earth (Hernández and Mesa, 2020). The elevated precipitation in this basin (Mesa S. and Rojo H., 2020) is due to the presence of a Walker cell convergence zone at the surface, persistent under neutral and La Niña conditions. This synoptic feature is one of the most important determinants of atmospheric circulation in Colombia, with prevailing east to west winds in the lower troposphere along with upper troposphere return winds (Mesa and Rojo, 2020). The Andean Cordilleras are nevertheless effective barriers to the Walker circulation near the CRV surface (Lopez and Howell, 1967; Mesa S. and Rojo H., 2020) (Lopez and Howell, 1967). The elevated humidity in the Pacific Ocean watershed and the closeness of the two Andes branches drive a zonal regional circulation pattern, consisting in of west to east anabatic winds over the Pacific slope of the Western Cordillera during daytime followed by rapid katabatic winds late afternoon (Lopez and Howell, 1967). These winds rapidly ventilate CRV during the late afternoon – early evening period on an almost regular basis. CRV is wide (~22 km) and long (~248 km) enough to develop a valley mountain wind circulation pattern during the daytime. Winds are very mild during this time period and expectedly highly dispersive, i.e. with high turbulence intensities (Ortiz et al., 2019). The arrival of the katabatic "tide" in the at late afternoon wipes the valley mountain wind pattern out (Lopez and Howell, 1967).

One year prior to the sampling period, we monitored the local meteorology, first at 14.5 m above the ground, a few meters over the mean canopy level, and then at 32.5 m above the ground during the sampling campaign. The box-and-whisker plot in Fig 2 shows katabatic tide winds of up to ~8 m/s at the sampling site elevation, peaking at ~17:00 LT. Wind speeds were a

factor ~2-3 slower at ground level. The wind runs at the sampling height were typically ~~over~~ above ~200 km per day (Fig S3) indicating that the samples had substantially broader ~~quite a large~~ spatial coverage of the CRV, much larger than it would have been at ground level. This also implies that the samples were frequently and significantly influenced by emissions coming from Yumbo's industrial hub (northwest of Palmira), and also by Palmira and Yumbo urban and highway emissions, as well as ~~along with~~ sugarcane PHB and sugarcane mill emissions. The wind rose (Fig 2a) suggests that the influence of urban emissions from Cali, the CRV's largest city by far, was minor. Other meteorological variables are reported in the Supplementary Material (SM) (Fig S2). Temperature (24.2ºC on average) and relative humidity (71.6%) were very likely controlled by solar radiation (350 W m^{-2} on average). The late-afternoon katabatic tide is fast enough to temporarily reduce the temperature. The daily pressure profile (~763 hPa on average) clearly showed the influence of the katabatic tide, with a ~3 hPa drop during its arrival in the ~~at~~ late afternoon. Overall, we believe our measurements at the Palmira site are reasonably ~~quite~~ representative of the regional air quality.

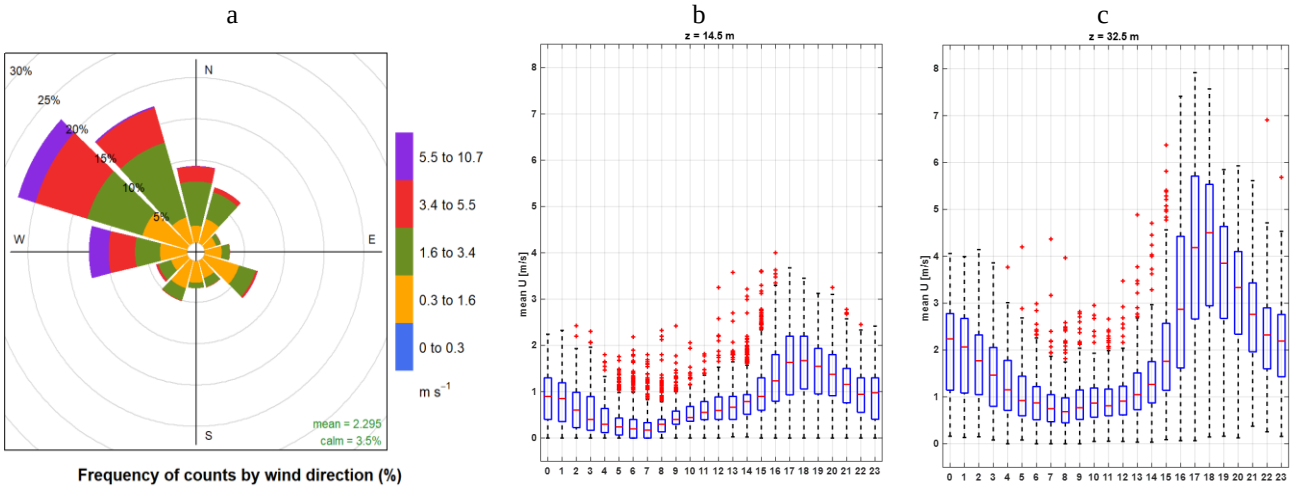

Figure 2. Wind pattern in the sampling location: a) predominant wind rose during the sampling period (July - September 2018), b) hourly profile of wind speed ~~to~~ at 14.5 m ~~over~~ above the ground (August – December 2017), and c) hourly profile of wind speed in sampling location at 32.5 m over the ground level (December 2017 – September 2018).

3.2. Bulk $PM_{2.5}$ concentration and composition

The daily $PM_{2.5}$ concentration measured in this study ranged from 6.73 to 24.45 µg m^{-3} with a campaign average of 14.38 ± 4.35 µg m^{-3} (23 h-average, ±1-sigma). Although these concentrations may appear comparatively low, it is worth stressing that samples were collected at more than 30 m height, with hourly wind speeds frequently above 4 m s^{-1}. However, most days during this study, $PM_{2.5}$ concentration exceeded the 5 µg m^{-3} annual mean and 15 µg m^{-3} 24-h mean guidelines by World Health Organization, (2021). Nevertheless, the Colombian standards are less demanding, thus observed concentrations comply with the 37 µg m^{-3} 24-h mean (MADS, 2017).

Previous studies conducted in rural areas of Brazil impacted by open field sugarcane burning reported significantly higher (mean 22.7 μg m^{-3}; Lara et al., 2005), similar (mean 18 μg m^{-3}Souza et al., 2014), and significantly lower $PM_{2.5}$ concentrations (mean 10.88 μg m^{-3}; Franzin et al., 2020). Comparable measurements in Mexico during harvest periods showed much higher concentrations, from 29.14 μg m^{-3} (Mugica-Alvarez et al., 2015) up to 51.3 μg m^{-3} (Mugica-Álvarez et al., 2016). Our $PM_{2.5}$ concentration measurements in the CRV are thus substantially lower than those usually reported in Mexico and Brazil during sugarcane burning periods. Major differences among sugarcane PHB practices in Colombia, Brazil and Mexico must be considered while comparing concentrations. First, the CRV currently burns "only" ~~in the CRV, "just"~~ ~1/3 of ~~the~~ its sugarcane area ~~is burned~~ before harvesting compared to much larger fractions in Mexico and Brazil (FAO, 2020). Second, in the CRV, sugarcane is harvested year-round, as opposed ~~in the CRV compared~~ to Brazil and Mexico, where harvest is limited to a ~6-month period (known in Spanish as *zafra* ~~in Spanish~~, "the harvest"). Third, the size of the individual plots burned in the CRV is typically ~6 ha (median burned area; Cardozo-Valencia et al., 2019), compared to much larger plots and total areas in Brazil and Mexico.

OC was the most abundant measured $PM_{2.5}$ component ~~of $PM_{2.5}$~~ with a mean daily concentration of 3.97 ± 1.31 μg m^{-3}, whereas the mean EC concentration was only 0.96 ± 0.31 μg m^{-3}. These two components contributed to 29.1 ± 8.3% and 7.2 ± 2.3% of the $PM_{2.5}$ mass, respectively (carbonaceous fractions were thus 4.93 ± 1.58 μg m^{-3}, i.e. 36.31 ± 10.41% of $PM_{2.5}$).

The most abundant water-soluble ions found in Palmira's $PM_{2.5}$ were SO_4^{2-}, NH_4^+, and NO_3, with average concentrations of 2.15 ± 1.39 μg m^{-3}, 0.67 ± 0.62 μg m^{-3}, and 0.51 ± 0.30 μg m^{-3}, respectively (12.7 ± 2.8%, 3.7 ± 1.1% and 2.6 ± 1.3% of mass concentration, respectively). ~~Mean concentrations of~~ Other water-soluble ions, such as Na^+, Ca^+, and $C_2O_4^{2-}$, had mean concentrations of ~~were~~ around 0.1 μg m^{-3}, while those of K^+, PO_4^{3-}, $CH_3O_3S^-$, Mg^{2+}, and Cl^- had concentrations ranging from ~~ranged within~~ 10-80 ng m^{-3} (Table 3).

The predominant elements were Ca (0.42 ±0.33 μg m^{-3}), K (0.13 ± 0.08 μg m^{-3}), and Fe (88 ± 65 ng m^{-3}), followed by Zn (34 ± 33 ng m^{-3}), Pb (18 ± 19 ng m^{-3}), Sn (52 ± 37 ng m^{-3}), Ti (5 ± 4 ng m^{-3}), Ba (9 ± 13 ng m^{-3}), Sr (2 ± 5 ng m^{-3}). Mn, Ni, Cr, and Se concentrations were below 2 ± 1 ng m^{-3}. Trace metals such as Ti, Cr, Mn, K, Ca, Fe, Ni, Cu, Zn Sr, Pb and Se were found in all $PM_{2.5}$ samples, while V was found only in a few samples. Other trace metals such as As and Sb were detected only at a reduced number of samples with concentrations below 20 ng m^{-3}. Table 3 shows the mean, standard deviation, minimum, and maximum concentration of the carbonaceous fraction, soluble ions, and metals found in the $PM_{2.5}$ samples collected in the CRV.

Table 3. Mean, 1 standard deviation, minimum and maximum concentrations of carbonaceous fraction, soluble ions, and metals in samples of $PM_{2.5}$ collected in Palmira.

Species	# of samples	Mean	SD	Min	Max	Units
$PM_{2.5}$	22	14.38	4.35	6.73	24.45	$\mu g\ m^{-3}$
OC	45	3.97	1.31	2.31	8.35	
EC	45	0.96	0.31	0.52	2.15	
SO_4^{-2}		2.15	1.39	0.98	10.27	
NH_4^+		0.67	0.62	0.18	4.29	
NO_3^-		0.51	0.30	0.11	1.45	
Na^+		0.21	0.16	0.02	0.45	
Ca^{+2} (Water soluble ion)		0.14	0.06	0.06	0.28	
$C_2O_4^{-2}$		0.11	0.06	0.04	0.36	
K^+ (Water soluble ion)		0.09	0.06	0.02	0.30	
Ca (Trace metal)		0.42	0.33	0.01	1.95	
K (Trace metal)		0.13	0.08	0.02	0.46	
Formate		82	88	0	217	$ng\ m^{-3}$
PO_4^{-3}		66	42	10	148	
Methansulfonate		50	36	13	256	
Cl-		20	19	0	75	
Mg^{+2}		19	10	2	52	
NO_2^-		3	1	1	6	
Fe		88	64	2	293	
Sn		52	37	9	137	
Zn		34	33	0	153	
Pb		18	19	0	84	
Ba		9	13	2	72	
Sb		8	5	3	22	
Cu		6	5	1	22	
Ti		5	4	0	17	
As		2	4	0	10	
Mn		2	1	0	5	
Ni		2	1	0	9	
Sr		2	5	0	28	
Cr		1	1	0	4	
Se		1	1	0	6	
V		0	1	0	3	

3.3. Ions

The SO_4^{2-} and NH_4^+ were the most abundant anion and cation in the $PM_{2.5}$ samples. The molar ratio between the most abundant cation and anion $[NH_4^+]/[SO_4^{2-}]$ was 1.6 ± 0.3 (min: 0.8 and max: 2.3). Acidic conditions in $PM_{2.5}$ can be inferred, since this ratio was less than two. To assess the acidity of the $PM_{2.5}$ samples, pH was calculated from of IV E-AIM thermodynamic model, in which the system conformed by H^+-NH_4^+-Na^+-SO_4^{2-}-NO_3^--Cl^--H_2O was parametrized to estimate the activity coefficient of these species in aqueous phase equilibrium. As result, the pH of $PM_{2.5}$ samples collected in the CRV was constant enough, with a mean of 2.5 ± 0.4. Despite the ions molar ratio do not is centered fact in the pH central concept, the correlation observed between $[NH_4^+]/[SO_4^{2-}]$ and pH was strong (r^2 = 0.96) as show in Figure S3 , which can help to understand the processes of gas - particle partitioning, acid catalytic reactions and metal dissolution that happen in the aerosols observed in CRV (Pye et al., 2020). Fine particles show a bimodal distribution of pH, with a population of particles having a mean pH of 1–3, and another population, influenced by dust, sea spray, and potentially biomass burning, having an average pH closer to 4–5 (Pye et al., 2020). In this study, just one $PM_{2.5}$ sample exceed a pH value of 4. Overall, this is an indicator of the abundance of sulfate and organics compounds in samples collected in the CVR.

The pH affects the partitioning of total nitrate (NO_3^- + HNO_3) and total ammonium (NH_4^+ + NH_3) between the gas and particulate phases. Lower pH values favor the partitioning of total nitrate toward the gaseous phase (HNO_3) rather than the particulate phase (NO_3^-). In contrast, the partitioning of total ammonium is favored toward the particulate phase, remaining as NH_4^+ over the aerosol, whereas SO_4^{2-} is a nonvolatile species that remained in the particulate phase. Acidity conditions in the samples collected in this study are consistent with concentrations of SO_4^{2-}, NH_4^+, and NO_3^-, corresponding to 2.5 μg m^{-3}, 0.7 μg m^{-3}, and 0.5 μg m^{-3}, respectively. Ammoniated sulfate and ammonium nitrate are generally considered the predominant forms of nitrate and sulfate in the inorganic fraction in fine particles. In limited environmental ammonium conditions, ammonia reacts preferentially with H_2SO_4 to form ammonium sulfate ($[NH_4]_2SO_4$), letovicite ($[NH_4]_3H[SO_4]_2$) or ammonium bisulfate ($[NH_4HSO_4]$) (Lee et al., 2008). Although the correlation coefficient between SO_4^{2-} and NH_4^+ concentrations was high (R^2 = 0.98), the amount of ammonium contained in the samples was not high enough to neutralize sulfate completely and form $[NH_4]_2SO_4$. In environmental with limited concentrations of ammonium, is expected the formation of sulfate salts not completely neutralized, as $[NH_4]_3H[SO_4]_2$ and $[NH_4HSO_4]$ (Ianniello et al., 2011). Thus, based on the limited ammonium concentrations found in $PM_{2.5}$ of CRV, the stoichiometric molar ratio between $[NH_4^+]/[SO_4^{2-}]$ of 3:2 for letovicite and 1:1 for ammonium bisulfate, and the results of the E-AIM model, it is possible to indicate that there is a mixture of sulfate salts, such as, ammonium bisulfate, letovicite, and ammonium sulfate, which is going to form progressively, according to ammonia availability. The E-AIM model presents the saturation ratio of each solid species, which usually forms before ammonium bisulfate than letovicite and ammonium sulfate. For a molar ratio of 1.5, the aerosol phase consists almost exclusively of letovicite and to form ammonium sulfate, the ratio should be over 2.0 (Seinfeld and Pandis, 2006).

The abundance amount of SO_4^{2-} can be attributed to oxidation of SO_2 and SO_3 emitted by from coal fired in power plants and industrial facilities (Wang et al., 2016), the biomass burning activities (Song et al. (2006)) and the emission of H_2S in poultry production animal production system (Casey et al., 2006). The H_2S emission from poultry and pork production is estimated using the factor emission given by animal units (AU) and the time that it stays in the housing, where one AU corresponding to 500 Kg of body mass. H_2S emissions from swine and poultry housing trend to be under 5 g H_2S AU^{-1} d^{-1} Casey et al., (2006), which can reach a 3.5 Ton H_2S d^{-1} by poultry and 5 Ton H_2S d^{-1} by pork production. Ammonia emissions factors by poultry and livestock vary from 0.09 to 12.9 AU^{-1} d^{-1} which represents 9.05 Ton NH_3 d^{-1} by poultry housing and 12. Ton d^{-1} by pork production.

In ammonia limited situations, NO_3^- might be bound to cations contained in sea salt and dust particles to form relative nonvolatile salts, as KNO_3, $NaNO_3$ and $Ca(NO_3)_2$. NO_3^- showed correlation with Na^+, Ca^{2+} and K^+ (r^2 = 0.6, 0.2 and 0.2, respectively), indicating possible formation of those salts. The correlation between Na^+ and NO_3^- could be explained by the impact of sea salt aerosol that comes from air mass origin in the Pacific Ocean. However, the amount of Na^+ is not enough to neutralize the total of NO_3^-, while Ca^{2+} showed to be enough amount to neutralize the NO_3^-. The molar ratio observed in $PM_{2.5}$ samples of CRV for $[NO_3^-]/[Ca^{2+}]$ was 2.6 ± 1.4, $[NO_3^-]/[Na^+]$ was 1.7 ± 1.3, and $[NO_3^-]/[K^+]$ was 5.0 ± 3.2, overcoming the stoichiometric molar ratio required to form $Ca(NO_3)_2$, $NaNO_3$, and KNO_3.

Methanesulfonate is produced predominantly by aqueous oxidation of dimethyl sulfide (DMS), one of the most abundant biogenic sulfur compounds in the troposphere. The oxidation of DMS is an important source of non-sea salt sulfate aerosol in marine and oceanic regions (Tang et al., 2019). Methanesulfonate is an organosulfur (OS) compound that can potentially impact the hygroscopicity and surface tension of particles and are useful tracers for secondary aerosol formation (SOA) (Sorooshian et al., 2015). This ion is one of the most easily measured OS species and its concentration can be used as a way of estimating the contribution of biogenic emissions on total sulfate levels. In addition to the oceanic source, methanesulfonate also has terrestrial sources, such as wetlands, freshwater lakes, alfalfa, ruminants, biomass burning, urban and agriculture emissions (Gondwe, 2004; Sorooshian et al., 2015). The [methanesulfonate]/$[SO_4^{2-}]$ ratio can be used to infer the origin of its compound and distinguish the impact of fires in the aerosols. In this study the [methanesulfonate]/$[SO_4^{2-}]$ ratio was 0.02±0.06 (min: 0.012 – max: 0.03), suggesting a minor impact of biogenic sulfur compared to the total inorganic sulfate concentration. However, the correlation between these two ions was very strong (r^2 = 0.88). This can be indicative of the existence of OS compounds, not included in this study, as part of the total sulfate levels. According to the average [methanesulfonate]/$[SO_4^{2-}]$ ratios presented by Sorooshian et al., (2015), coastal regions exhibit higher values (0.06 to 0.09) than inland regions (0.02-0.04). It is then possible to suppose that high methanesulfonate concentrations in the CRV were derived from continental sources. This is supported by the non-existent correlation between Na^+ and methanesulfonate, and the moderate correlation between $C_2O_4^{2-}$ and methanesulfonate (r^2 = 0.66). Even though the air mass from the Pacific Ocean has an impact on winds

that ventilate the CRV in the late afternoon, the western mountain range may act as a barrier for an important fraction of sea salt aerosol.

~~Anion- and cation equivalent (AE and CE, respectively) charges were compared to estimate the acidity of $PM_{2.5}$ (¡**Error! No se encuentra el origen de la referencia.**). AE and CE displayed a tight Spearman linear correlation (r^2=0.99). The AE to CE ratio of 1.2 ± 0.1 suggests that cations were generally well balanced by anions and that $PM_{2.5}$ was nearly neutral. Just a few samples displayed AE/CE ratios significantly higher than 1, i.e. slightly acidic, which might be attributed to the sulfate dianion (SO_4^{2-}) abundance. The ratio between the two main water soluble ions, ammonium cation (NH_4^+) and SO_4^{2-}, was $[NH_4^+]/[SO_4^{2-}]$ = 0.3 ± 0.1 This indicates that fine PM in CRV is more acidic than suggested by the AE/CE ratio. This acidity might be explained by insufficient ammonium in CRV's atmosphere to neutralize SO_4^{2-} present in fine particulate matter.~~

~~Sulfate to nitrate ratios ($[SO_4^{2-}]/[NO_3^-]$) have been used as indicators of the relative contribution of mobile and stationary sources to particulate matter nitrogen and sulfur (Agarwal et al., 2020; Begam et al., 2016). High values indicate the dominance of stationary sources over vehicular emissions.~~ The measured average ratio of $[SO_4^{2-}]/[NO_3^-]$ = 4.5 ± 2.9 ~~indicates that stationary sources are predominant in the CRV~~. This ratio is higher than the one obtained ~~in Brazil~~ by Souza et al. (2014) at Piracicaba (3.6 ± 1.0) and Sao Paulo (1.8 ± 1.0), Brazil. The strong correlations between SO_4^{2-} and NH_4^+ (r^2 = 0.98), SO_4^{2-} and methanesulfonate ($CH_3O_3S^-$) (r^2 = 0.88), and SO_4^{2-} and oxalate dianion ($C_2O_4^{2-}$) (r^2 = 0.71) allow us to infer that inorganic secondary aerosol formation is a significant $PM_{2.5}$ source in the CRV. In addition, the presence of potassium cation (K^+) in submicron particles is recognized as a biomass burning tracer (Andreae, 1983; Ryu et al., 2004). K^+ showed a moderate correlation with nitrite anion (NO_2^-) (r^2 = 0.44) and $C_2O_4^{2-}$ (r^2=0.43) in the CRV, which suggests that biomass burning influences secondary aerosol formation. Mg^{2+} and Ca^{2+} ions, usually considered crustal metals, exhibited a moderate correlation of r^2 = 0.64 (Li et al., 2013). Also, Mg^{2+} and $C_2O_4^{2-}$ moderate correlation (r^2 = 0.26) points to a link ~~among~~ between crustal species and secondary aerosols. Such an association could be plausibly explained by soil erosion induced by pyro-convection during sugarcane pre-harvest burning (Wagner et al., 2018). Our study full species correlation matrix is shown in Fig 4S.

3.4. Metals

The measured total $PM_{2.5}$ trace metal concentration was 706 ± 462 ng m^{-3} (101.3 ng m^{-3} to 2638 ng m^{-3}). Trace metals can originate from non-exhaust and exhaust emissions. ~~The n~~ Non-exhaust emissions come from brake and tire wear, road surface abrasion, wear/corrosion of other vehicle components, and the resuspension of road surface dust (Pant and Harrison, 2013). Metals in e~~E~~xhaust emissions ~~metals~~ are related to fuel, lubricant combustion, catalytic converters, and engine corrosion. As shown by Kundu and Stone (2014), many of these sources share some metals in their chemical composition profile, thus an unambiguous specific source attribution is non-trivial. In this study, we found a significant correlation among Fe, Mn and Ti

($r^2 \approx 0.72$), which is typically associated with a high abundance of crustal material (Fomba et al., 2018), and substantiates the importance of soil dust as a significant source in the CRV. Also, tire and brake wear tracer metals, including Zn and Cu, showed weaker but still significant correlations among them ($r^2 \approx 0.32$). ~~$PM_{2.5}$~~ Ca concentrations ~~at Palmira~~ were quite high (405 ± 334 ng m^{-3} (1.6 ng m^{-3} to 1952 ng m^{-3}). These levels can be attributed to dust generation by agricultural practices, particularly land planning, liming and tilling, PHB pyro-convection-induced soil erosion, and traffic-induced soil resuspension on unpaved rural roads. One of the very few previous investigations into on PM composition in the CRV (Criollo and Daza, 2011) analyzed trace metals in PM_{10} at 4 CRV locations, including Palmira. They found significant enrichment of Fe and K metals at locations exposed to PHB. It must be kept ~~bear borne~~ in mind that PM_{10} samples included coarse mode aerosols, of which dust might have been a significant fraction. Also, environmental regulations have been successful in steadily reducing the sugarcane burned area in the CRV since 2009. The Burned area dropped from 72% in 2011 to 35.46% in 2018, our year of measurements (Cardozo-Valencia et al., 2019).

Cd, Pb, Ni, Hg and As, and other metals and metalloids are considered carcinogenic (WHO Regional Office for Europe, 2020). Measured concentrations of Pb and Ni in $PM_{2.5}$ at Palmira were 18 ng m^{-3} (+/-19) and 2 ng m^{-3} (+/-1), respectively. These mean values were below the EU target values of (0.5 μg m^{-3} and 20 ng m^{-3} respectively) (WHO, 2013a), and below the annual average limit of the Colombian national ambient air quality standard (0.5 μg m^{-3} and 0.18 μg m^{-3} respectively) (MADS, 2017). Nevertheless, these concentrations are ~~nevertheless~~ significantly higher than those reported for other suburban areas in Midwestern United States and remote sites in the northern tropical Atlantic (Fomba et al., 2018; Kundu and Stone, 2014). Pb concentrations are similar to those reported for Bogota and other large urban areas (SDA, 2010; Vasconcellos et al., 2007). Pb has been long banned as a fuel additive in Colombia, thus the observed levels might be associated with metallurgical industry and waste incineration. Information on ambient air hazardous metal concentrations in Latin America's urban and rural areas is still scarce.

3.5. Carbohydrates

Levoglucosan is a highly specific biomass burning organic tracer (Bhattarai et al., 2019). Along with K^+, OC and EC, it can be used to effectively identify the relevance of biomass burning as an aerosol source. The relative contribution of levoglucosan to the PM carbohydrate burden, and especially the levoglucosan to mannosan ratio, can be used as indicators of the type of biomass burned (Engling et al., 2009). In this study, the following carbohydrates were quantified: levoglucosan, mannosan, glucose, galactosan, fructose and arabitol. Levoglucosan was by far the most abundant (113.8 ± 147.2 ng m^{-3}), reaching values of up to 904.3 ng m^{-3}, followed by glucose (10.4 ± 6.1 ng m^{-3}), mannosan (7 ± 6.1 ng m^{-3}), and arabitol (4.1 ± 3.5 ng m^{-3}). Levoglucosan and mannosan were detected in all $PM_{2.5}$ samples, while galactosan and fructose were detected only in 9 and 11

~~a very reduced~~ ~~number of~~ samples, respectively. Levoglucosan was ~~accounted for~~ 3.5±2.3% of OC and 0.96% ± 0.81% of $PM_{2.5}$.

The levoglucosan concentration found in this study was quite similar to that ~~the~~ reported in areas of Brazil where sugarcane production and processing are important economic activities. For instance, during the harvest (*zafra*) period in Araraquara, the levoglucosan mean concentration was 138 ± 91 ng m^{-3}, although during the non-harvest period it was unexpectedly high (73 ± 37 ng m^{-3}) (Urban et al., 2014). Likewise, the levoglucosan average concentration at Piracicaba during a reduced fire period was 66 ng m^{-3} (Souza et al., 2014). The measured mean levoglucosan/mannosan ratio in Palmira was 17.6 ± 13.0 (min: 8.1 – max: 58.1). Chemical profile studies found a levoglucosan/mannosan ratio of ~10 for sugarcane leaves burned in stoves (Hall et al., 2012; Dos Santos et al., 2002) and of ~54 for burned bagasse (Dos Santos et al., 2002). Leaves constitute the largest fraction (20.8%, Victoria et al., 2002) of pre-harvest burned sugarcane. Consistently and expect~~edly~~ably, the levoglucosan/mannosan ratio at Palmira is much closer to the chemical profile ratio of leaves than that of bagasse. Moreover, ambient air samples in Araraquara and Piracicaba showed levoglucosan/mannosan ratios of 9 ± 5 and ~33, respectively. For comparison, the levoglucosan/mannosan ratio in PM from rice straw and other crops burn~~ing~~ed was were ~26.6 and~23.8, respectively (Engling et al., 2009). This indicates that the levoglucosan/mannosan ratio is sensitive to the type of biomass burned but also to burning conditions. The large levoglucosan/mannosan ratio ~~variability~~ in our study suggests that Palmira was impacted by sugarcane PHB most of the time ~~but also~~, and, to a lesser extent, by bagasse combustion in sugar mills ~~to a lesser extent~~. So far, Levoglucosan and mannosan emissions factors from bagasse combustion have not been reported ~~so far~~. We hypothesize that, even if these were very small, levoglucosan and mannosan combustion emissions might not be negligible ~~negligeable~~ as the CRV sugarcane biomass yields are very high and most of the harvested sugarcane bagasse is combusted for electric power and steam production.

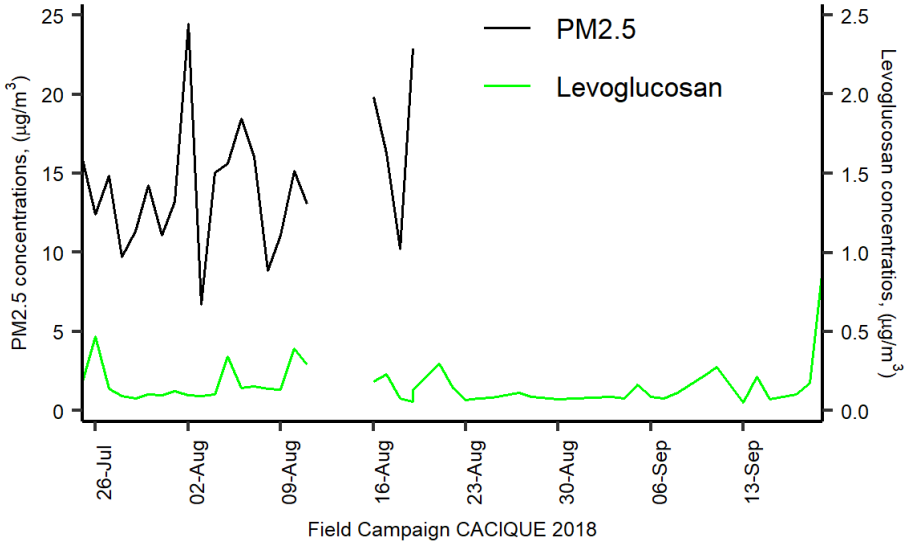

Figure 3.Daily variation of Levoglucosan and PM2.5 concentration at CRV.

3.6. Polycyclic Aromatic Hydrocarbons (PAH)

A total of 22 PAH~~s~~ were measured in each sample collected at Palmira, including the 16 PAH~~s~~ listed as human health priority pollutants by WHO and US-EPA (Yan et al., 2004). The total PAH concentration was 5.6 ± 2.9 ng m^{-3} (min: 2.3 ng m^{-3} – max: 15.8 ng m^{-3}). Figure 4a shows the PAH concentration variability during the sampling campaign (mean and standard deviation are available in Table S2). The most abundant PAH were FLE (44.2%±11.9% total concentration share), ANT (9,10) (10.0%±4.5%), BbF (7.4%±2.3%), BghiP (6.7%±2.4%), IcdP (6.4%±1.9%), CPY (6.0%±2.3%), FLO (9H) (5.4%±3.1%), BeP(4.6%±1.3%), and BaP(4.4%±1.6%), which accounted for 95.1% of the total PAH concentration (Figure 4b). Three-ring PAH~~s~~ were the most abundant (59.04% of total PAH). Put together, five- and six-ring PAH~~s~~ accounted for an additional 38.44%. The less abundant PAH group was the four-ring (2.52%). A previous study in CRV, carried out on PM_{10} samples by Romero et al. (2013), ~~but on PM_{10} samples,~~ showed higher FLT, PYR, and PHE concentrations in areas highly exposed to sugarcane PHB compared to other locations. In contrast, $PM_{2.5}$ FLE concentrations in this research were significantly higher than those in PM_{10} by Romero et al. (2013), while PYR and PHE levels were similar.

The carcinogenic species BaP, BbF, BkF, BaA, BghiP, FLE, CPY and BeP were identified in all the $PM_{2.5}$ samples. BaP is a reference for PAH carcinogenicity (WHO, 2013a) that is used as a PAH exposure metric, known as the BenzoaPyrene-equivalent carcinogenic potency (BaPE). We calculated BaPE using the toxic equivalent factors (TEF) proposed by Nisbet and LaGoy (1992) and (Malcolm and Dobson, 1994). PAH concentrations were multiplied by TEF and then added to estimate the carcinogenic potential of $PM_{2.5}$-bounded PAH. The mean carcinogenicity level at Palmira, expressed as BaP-TEQ, was 0.4

675 ± 0.2 ng m^{-3} (min: 0.1 ng m^{-3} - max: 1.4 ng m^{-3}). Only one sample exceeded the Colombian annual limit of 1 ng m^{-3} but most
676 of them exceeded the WHO reference level of 0.12 ng m^{-3}. The mutagenic potential of PAH (BaP-MEQ) was estimated using
677 the mutagenic equivalent factors (MEF) reported ~~for~~ by Durant et al., (1996). The average BaP-MEQ was 0.5 ± 0.3 ng m^{-3}
678 (min: 0.2 ng m^{-3} - max: 1.8 ng m^{-3}). These levels are comparable to those measured in $PM_{2.5}$ by Mugica-Álvarez et al., (2016)
679 in Veracruz (Mexico) but during the sugarcane non-harvest period. PM_{10} BaP-MEQ levels in Araraquara (Brazil) (de Andrade
680 et al., 2010; De Assuncao et al., 2014) were twice as high as those found in this study. This suggest~~s~~ that year-long sugarcane
681 PHB in the CRV leads to lower mutagenic potential~~s~~ compared to those at locations where the harvesting period (*zafra*) is
682 shorter, thus with higher burning rates. We estimated the average BaP-TEQ and BaP-MEQ concentrations in the CRV
683 according to their exposure to sugarcane burning products from Romero et al., (2013) data and used them as a benchmark to
684 our measurements. PM_{10}-bound BaP-TEQ and BaP-MEQ levels for areas not directly exposed to sugarcane burning were 0.16
685 ng m^{-3} and =0.21 ng m^{-3}, respectively. Toxicity and mutagenicity due to PM_{10}-bound PAH~~s~~ were ~~a factor~~ 4 times ~~higher~~ as
686 high as those at areas directly exposed to sugarcane burning. It is reasonable to assume that PAH~~s~~ are largely bound to fine
687 aerosol (<2.5 µm), thus that our measurements are comparable to (Romero et al., 2013). If so, our site at Palmira would be at
688 an intermediate exposure condition, higher than areas not directly exposed to sugarcane burning but lower than directly
689 exposed areas.
690
691 Ratios among different PAH~~s~~ have been extensively used to distinguish between traffic and other PAH sources. We used the
692 diagnostic ratios presented by Ravindra et al. (2008) and Tobiszewski and Namieśnik (2012a) to better understand the
693 contribution of sources to $PM_{2.5}$ in the CRV. The ratio benzo(e)pyrene ~~ratio~~ to the sum of benzo(e)pyrene and benzo(a) pyrene
694 is used as an indicator of aerosol aging ~~indicator~~. Local or "fresh" aerosols have [BeP]/([BeP]+[BaP]) ratios around 0.5, while
695 aged aerosols can have ratios as low as zero as a result of photochemical decomposition and oxidation. The
696 [BeP]/([BeP]+[BaP]) ratio at Palmira was 0.51 ± 0.04, with a majority (84.4%, n = 38) of fresh samples a minor fraction
697 (15.6%, n=7) of photochemically-degraded samples.
698
699 Other two diagnostic ratios were used to assess the prevalence of traffic as a $PM_{2.5}$ source. The first ratio ~~one~~ used IcdP ~~and~~
700 BghiP, two automobile emissions markers (Miguel and Pereira, 1989). Values higher than 0.5 for the ~~IcdP~~ ratio ~~to the sum of~~
701 ~~IcdP and BghiP,~~ [IdcP]/([IdcP]+[BghiP]) indicates aged particles (Tobiszewski and Namieśnik, 2012) generated by coal, grass
702 or wood burning (Yunker et al., 2002). The second ratio is [BaP]/[BghiP]. Ratios higher than 0.6 are indicative of traffic
703 emissions (Tobiszewski and Namieśnik, 2012). At Palmira, the [IdcP]/([IdcP]+[BghiP]) and [BaP]/[BghiP] ratios were 0.48 ±
704 0.04 and 0.69 ± 0.13, which indicates that ~63% of the samples originated from combustion of oil products (n = 30), and ~36%
705 came from non-traffic sources, like wood, grass, or coal (n = 15).
706

Also, the structure and size of PAH~~s~~ are indicative of their sources. PAH~~s~~ ~~with~~ of low molecular weight (LMW) (two or three aromatic rings) ~~has~~ have been reported as tracers of wood, grass, and fuel oil combustion, while ~~the PAHs~~ those of medium molecular weight (MMW) (four rings) and high molecular height (HMW) (five and six rings) are associated with coal combustion and vehicular emissions. The ratio between LMW ~~ratio~~ ~~to~~ and the sum of MMW and HMW, LMW/(MMW+HMW), is used for source identification. Ratios lower than one are indicative of oil product~~s~~ combustion, while ratios larger than one are associated ~~to~~ with coal and biomass combustion (Tobiszewski and Namieśnik, 2012). The ratio at Palmira, LMW/(MMW+HMW) = 1.43 ± 1.00, was rather variable but suggests that a large fraction of PAHs in ~~the~~ CRV (82.2% of samples) were generated by biomass burning or combustion, as coal combustion is quite limited nowadays. Just one in five samples (17.8%) had PAH~~s~~ attributable to oil product~~s~~ combustion.

Sugarcane-burning emitted PAH~~s~~ are mainly LMW ~~of low molecular weight~~, especially of two (~66% of PAH) and three rings (~27%), among which FLE, PHE and ANT are the most emitted, according to Hall et al. (2012) chemical profile. The relative abundance of three-ring PAH~~s~~ (Figure 4) in CRV's $PM_{2.5}$ is likely due to open-field sugarcane PHB to a major extent, and to controlled bagasse combustion for electric power and steam production~~,~~ to a lesser extent.

The highest PAH concentrations ~~of PAH~~ were observed on 10th August and 11th September 2018, with levels of 15.8 ng m^{-3} and 14.4 ng m^{-3}, respectively (Fig 5S). In particular, ~~on 10th August 2018~~ elevated concentrations of 5 and 6 ring~~s~~ PAH~~s~~ were observed on 10th August 2018. ~~a~~ A change in the wind circulation pattern ~~form~~ was observed on the previous day ~~on~~ (Fig S2), with a wind speed reduction and a predominance of winds from the north. ~~Then~~ Later, on 11th September 2018, we observed an increase in ~~of~~ 3-ring PAH~~s~~ and winds from the NW at the average wind speed at the sampling location. This indicates that there were at least two types of sources. The abundance of HMW PAH~~s~~ indicates fossil fuel combustion sources, and LMW PAH~~s~~ suggests that parts of these come from non-fossil fuel combustion sources.

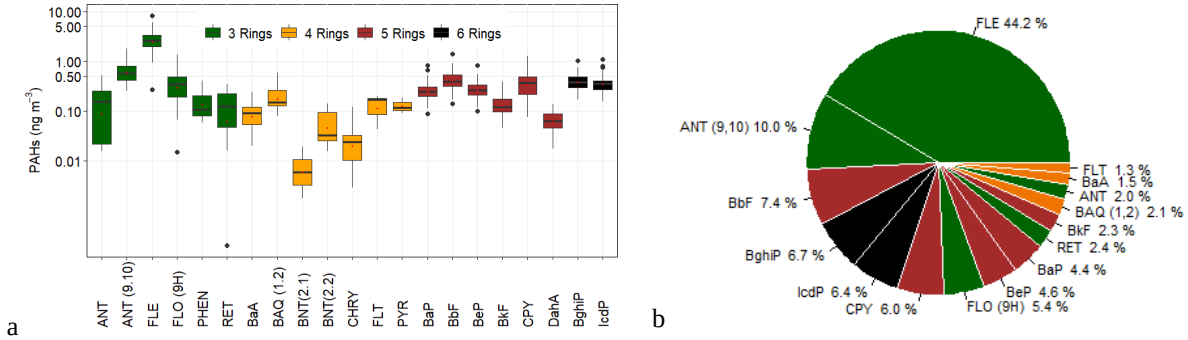

Figure 4. ~~A~~ The abundance of PAH~~s~~ measured in $PM_{2.5}$ samples collected in CRV, represented by colors according to the number of rings of each PAH, green (tree rings), yellow (four rings), brown (five rings), and black (six rings). a) Box~~-~~plot of

concentrations in ng m^{-3}, red dots represent mean concentrations of each PAH. b) pie-plot of the relative abundance of PAH~~s~~ in $PM_{2.5}$ samples.

3.7. Alkanes

A total of 16 alkanes ranging from C_{20} up to C_{34} were analyzed in this study and used to identify the presence of fossil fuel combustion and plant fragments in the $PM_{2.5}$ samples. The abundance of total n-alkanes during the whole sampling period was in the range of 13.0 to 88.45 ng m^{-3} with an average concentration of 40.36 ng m^{-3} ± 18.82 ng m^{-3}. In general, the high molecular weight n-alkanes such as C_{29} – C_{31} were the most abundant. These are characteristic of vegetative detritus corresponding to plant fragments in airborne PM ~~particle matter~~ (Lin et al., 2010). The most abundant n-alkanes were C_{29}, C_{30}, and C_{31} (Fig 6.). Likewise, the carbon number maximum concentration (C_{max}) was C_{29} in 43% of samples and C_{31} in 28% of them. This result is consistent with the chemical profile of sugarcane burning reported by (Oros et al., 2006) with a C_{max} of C_{31}.

The carbon preference index (CPI) and wax n-alkanes percentage (WNA%) are parameters used to elucidate the origin of the n-alkanes and infer whether emissions come from biogenic or anthropogenic sources. The CPI represents the ratio between odd and even carbon number n-alkanes. The equation used to calculate CPI in the present study is shown in Table 2, following the procedure reported by (Marzi et al., 1993). Values of CPI ≤ 1 (or close to 1) indicate that n-alkanes are emitted from anthropogenic sources, while values higher than 1 indicate the influence of vegetative detritus and biomass burning in the $PM_{2.5}$ samples (Mancilla et al., 2016). In this study, the mean CPI was always greater than 1, with an average value of 1.22 ± 0.18 (min:1.02 – max:1.8) that is between the CPI for fossil fuel emissions of ~1.0 (Caumo et al., 2020) and sugarcane burning of 2.1 (Oros et al., 2006), revealing the influence of several sources over the $PM_{2.5}$ in the CRV.

Likewise, WNA% represents the preference of odd n-alkanes in the sample. The odd n-alkanes, especially of higher molecular weight, are representative of plant wax related emissions. The waxes are present on the surface of plants, especially on the leaves, and they become airborne by a direct or indirect mechanism like wind action or biomass burning (Kang et al., 2018; Simoneit, 2002). In this research, the samples analyzed showed a preference for odd carbon on C_{27}, C_{29}, C_{31} and C_{33}, which have higher concentrations than the next higher and lower even carbon number homologs, proving the biogenic contribution over the $PM_{2.5}$ in the CRV. The WNA% was calculated using the equation shown in Table 2, described by Yadav et al. (2013). A larger WNA% represents the contribution from emissions of plant waxes or biomass burning. Otherwise, a smaller value represents ~~that~~ n-alkanes from petrogenic sources, known as petrogenic n-alkanes (PNA)%. The mean WNA% calculated for the $PM_{2.5}$ samples collected from the CRV was 12.65% ± 5.21% (min: 4.71% – max: 29.92%) and can be defined as petrogenic inputs (PNA%) that were 87.35% during the sampling period. The correlation between CPI and WNA was moderate (r^2=0.53) supporting a consistent meaning between these two parameters, and they are useful for assessing the plant wax contribution ~~on~~ to $PM_{2.5}$.

Overall, the total concentration of n-alkanes ~~of~~ in the $PM_{2.5}$ in the CRV was lower than those reported in areas where ~~the~~ sugarcane is often burned in Brazil (Urban et al., 2016), although the behavior of the parameters of CPI and C_{max} is similar. Compared with other urban areas in Latin America~~n~~, the n-alkane concentration in the CRV was similar to that reported in the metropolitan zone of the Mexican valley (MZMV) for $PM_{2.5}$ (Amador-Muñoz et al., 2011), ~~and~~ Bogota for PM_{10} and slightly lower than reported in Sao Paulo for PM_{10} (Vasconcellos et al., 2011). However, the CPI and WNA in these cities were smaller than in the CRV, because of the strong influence of vehicular emissions in these densely populated cities. The OC/EC ratio was moderately associated with WNA values (r^2 = 0.41), indicating that an increase ~~on~~ in this ratio can be explained by the vegetative detritus contribution to ~~in the~~ $PM_{2.5}$, while the levoglucosan concentrations did not show correspondence to the CPI and WNA values; therefore, the levoglucosan levels did not explain the preference of odd carbon number homologs. These results indicated that the n-alkanes found in this study came from several sources, with a noticeable contribution from plant wax emissions. The parameters used to assess the source contribution of $PM_{2.5}$ through n-alkanes such as CPI and WNA%, were characteristic of aerosols collected in urban areas.

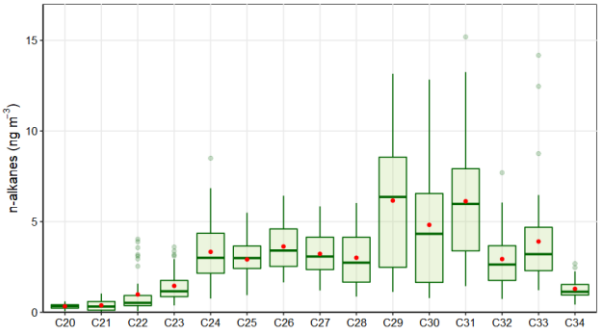

Figure 5. Average n-alkanes concentrations in $PM_{2.5}$ samples

3.8. $PM_{2.5}$ mass closure

~~The m~~ Mass closure (Figure 6) shows the crucial contribution of organic material (~~52.99~~ 52.66 ± ~~17.79~~18.44%) and ~~the secondary~~ inorganic fraction, represented by ~~ammoniated~~ sulfate ~~sulphate~~ (~~16.12~~ 12.69 ± ~~3.98~~2.84%), ~~and~~ ammonium (3.75 ±1.05%) ~~and~~ nitrate (~~3.19~~ 2.56±~~1.71~~1.29%). EC constituted ~~6.95~~ 7.13% ± ~~2.52~~2.44% of $PM_{2.5}$. The mineral fraction corresponded to dust (~~8.67~~ 3.51± ~~5.71~~ 1.35%) and TEO (~~0.82~~ 0.85 ± ~~0.44~~ 0.42%). ~~The sea salt was 0.80 ± 1.28 % and PBW 5.20 ± 1.20%.~~ A mass closure of ~~93.40~~ 88.42± ~~33.38~~24.17% was achieved. Although ~~the~~ $PM_{2.5}$ concentrations observed in the CRV were not so high as compared with those registered in Brazil and Mexico during the preharvest season, the EC percentage is in a similar range or slightly lower than those observed in other urban areas (Snider et al., 2016), showing the key role of incomplete combustion processes in the area.

The average (OC/EC) ratio found in CRV was 4.2 ± 0.72, from which we can infer that secondary aerosol formation had a relevant role. The segregation of OC into the primary and secondary fractions was ~~made~~ carried out using two methods: first was the EC tracer method applied in previous studies (Pio et al., 2011; Plaza et al., 2011), and a second method based on the lineal regression between OC and organic tracers from primary sources. In the EC tracer method, the $(OC/EC)_{min}$ ratio selected to differentiate OC_{prim} from OC_{sec} was the minimum ratio observed, equivalent to 2.12. Still, this value could induce the overestimation of OC_{prim} due to the distance between the emission sources and the sampling site (27 m ~~overground~~ aboveground), and ~~by~~ the local meteorological conditions that favor the volatilization and oxidation of organic components into particles before being collected. As a result, OC_{prim} was estimated ~~as~~ at 50.3% and OC_{sec} ~~as~~ at 49.7% ~~over~~ of the total OC, with a minimum variability of 3.8%. The estimated OM_{pri} concentration was ~~2.95~~ 3.22± 1.0~~95~~ μg m^{-3} and the OM_{sec} concentration was 4.0~~18~~ ± 1.78~~86~~ μg m^{-3} ~~that~~,-which represented ~~the~~ 24.2% and 28.5% of $PM_{2.5}$ respectively.

The contribution of fossil fuel, mainly derived of traffic combustion, biomass burning, and vegetative detritus to OC_{prim} was estimated from a linear relationship between organic tracers and OC. Resulting contributions were as follows: OC_{ff}: 16.38%, OC_{bb}: 15.19%, and OC_{det}: 1.45%. Overall, the use organic tracer method to estimate OC_{prim} indicates that this carbonaceous fraction represents 32.68% ± 11.02% of total OC, and it may fluctuate between 17.61% and 68.60%. The difference between OC_{prim} from the organic tracer method and that obtained from the EC tracer method can be associated to the fact that the organic tracer method may not be representative of all sources. Industrial coal and fuel oil burning, garbage burning, cooking, charcoal production and other sources may not be accounted for by this method. This can be estimated through use of organic tracers specific of this kind of activities no available on this study. Using $C_2O_4^{2-}$ and methansulfonate as tracers of the formation OC_{sec} on a linear model was estimated that it fractions corresponding to 34.36% ± 8.11% with a variation from 19.00 % – 58.20 %.

The use of the organic tracers' method to apportionment OC_{prim} and OC_{sec} was consistent with the distribution obtained from EC tracer method. The mass reconstruction fraction resulting from the organic tracers' method was 70.89 ± 18.4% while using the EC tracer method was 88.42 ± 4.17%.

The mineral fraction, quantified as the sum of the oxides present in the crustal material (dust) and other TEO contributed 3.51~~9.1~~ ± 1.35~~5.5~~% and 0.85 ~~0.9~~ ± 0.42%, respectively. Despite the non-quantification of highly abundant mineral dust elements such as Si, the concentrations of Ca, Ti, and Fe indicated the impact of soil resuspension on the $PM_{2.5}$ mass concentration.

PBW depends on the concentration of hygroscopic compounds embodied in the PM and the relative humidity of the weighing room where ~~the~~ $PM_{2.5}$ mass collected on the filters was determined. In this study, it was assumed that (i) NH_4^+, SO_4^{2-} and NO_3^- were the main compounds responsible for ~~the~~ absorbed water and (ii) thermodynamic equilibrium is dominated by these ions that allow calculating the H^+ molar fraction as a difference ~~of~~ between (SO_4^{2-}+ NO_3^-) and NH_4^+, which is required to establish ~~the~~ charge neutrality. Polar organic compounds and other water-soluble ions were not considered in the present study. The PBW content was estimated using the mean measured concentrations of NH_4^+, SO_4^{2-} and NO_3^- in the AIM Model, where a multiplier factor ~~was found equivalent to~~ of 0.32 was found as a proportion between the concentrations of the sum~~matory~~ of these ions and the water fraction contained in ~~the~~ $PM_{2.5}$. As a result, ~~the~~ PBW was 5.3% of the $PM_{2.5}$ mass concentration.

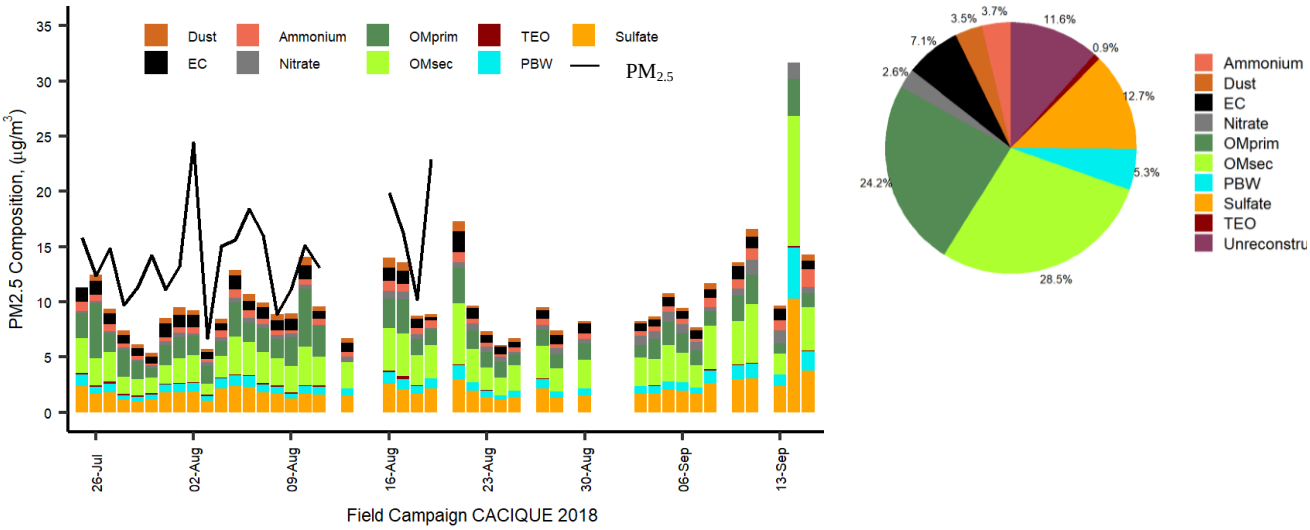

Figure 6. Mass reconstruction of $PM_{2.5}$ collected in CRV. Figure in left corresponding to timeseries of $PM_{2.5}$ gravimetric mass measured and reconstructed mass from the chemical speciation in CRV during July – September 2018 and right is the to pie plot the relative mean contributions (%) of major chemical components of gravimetric PM2.5 based on chemical speciation.

~~3.9. PCA~~

~~We applied a PCA to the chemical composition data to assess the latent factors controlling the $PM_{2.5}$ concentrations in the CRV. This statistical tool was used to find the chemical species that describe each component and qualitatively associate these to potential sources of fine aerosol particles. In order to extract the number of components in a PCA many procedures exist, while one of the most common ones is the scree plot of successive eigenvalues for several components from which it is possible to identify the point where the proportion of the variance explained by each subsequent component drops off abruptly. Fig S7 shows the inflection point in component number four, explaining 45% of the chemical composition data variance. The addition~~

of two following components allows describing 61% of the variance. Therefore, this study was conducted taking into account six components. Table 4 shows the loading for each chemical component assessment for the six components, where the loadings higher than 0.6 were considered in the discussion interpreted as a source that contributed to the formation of $PM_{2.5}$.

Table 4. Loading of PCA after varimax rotation. Loading with |x| < 0.2 was considered insignificant and removed, while loading |x| < 0.6 is considered high and is **printed bold.**

Principal Component	PC1	PC2	PC3	PC4	PC5	PC6
Potential Source	Road dust resuspension	Secondary aerosols and biomass burning	Fuel Combustion 1	Detritus vegetables	Fuel Combustion 2	Agricultural soil resuspension
% variance explained	13	11	11	10	9	7
% cumulative variance	13	24	35	45	54	61
OC	0.26	**0.66**	0.34	0.33	0.34	0.2
EC	-	**0.73**	0.39	-	0.37	-
$C_2O_4^{2-}$	-	**0.65**	-	0.52	-	0.39
K^+ (Water soluble ion)	-	0.39	-	**0.69**	-	0.3
NO_2^-	-	**0.65**	0.23	0.43	-	-
F^-	-	0.32	-	0.36	-	-
NO_3^+	-	0.41	-	-	-	**0.64**
Cl^-	-	-	-	-	-	**0.61**
Ca^{2+} (Water soluble ion)	-	0.29	-	-	-	**0.74**
NH_4^+	-	**0.87**	-	-	-	-
SO_4^{2-}	-	**0.88**	-	-	-	0.26
Formate	-	-	-	0.34	-	0.25
Na^+	-	0.33	-	-	0.25	0.36
Mg^{2+}	-	0.24	0.21	-	-	**0.77**
Methansulfonate	-	**0.81**	-	0.23	-	-
PO_4^{3-}	-	0.38	-	-	-	-
Cr	-	-	-	-	-	-
Ca	**0.63**	-	-	-	0.2	0.41
K	0.43	0.2	-	**0.62**	0.2	-
Ti	0.39	-	-	-	-	-
Fe	**0.74**	0.35	-	-	-	-
Sb	0.58	-	-	-	-	-

Mn	0.46	0.26	-	-	-	-
Ba	**0.73**	-	0.25	-	-	-
Se	0.40	0.55	-	-	-	-
Zn	**0.80**	-	-	-	-	-
As	-	0.57	-	-	-	-
Sr	0.37	-	-	-	-	-
Pb	0.24	0.42	-	-	-	-
Sn	**0.61**	-	0.25	-	0.35	-
Cu	0.52	0.24	0.3	-	-	-
Ni	0.3	0.25	-	-	-	-
C20	-	-	0.33	-	0.29	0.29
C21	0.51	-	0.29	-	0.32	-
C22	-	-	-	-	**0.85**	-
C23	0.3	-	-	-	**0.84**	-
C24	-	-	0.43	0.25	**0.67**	-
C25	-	-	-	-	**0.84**	-
C26	-	-	0.34	0.33	**0.78**	-
C27	-	-	0.29	0.53	**0.65**	-
C28	-	-	0.24	**0.62**	0.48	0.26
C29	-	-	-	**0.69**	0.33	0.26
C30	-	-	-	**0.68**	0.32	0.21
C31	-	-	-	**0.78**	0.3	-
C32	-	-	-	**0.76**	-	-
C33	-	-	-	**0.79**	-	-
C34	-	-	-	**0.65**	-	-
FLT	-	-	-	-	-	-
PYR	-	-	-	-	-	-
BNT (2,1)	-	-	-	-	-	-
RET	0.33	-	-	-	-	-
PHEN	-	0.46	-	-	-	0.28
BAQ (1,2)	-	-	-	-	-	-
ANT	-	0.47	-	-	-	0.27
DahA	0.48	-	0.42	-	-	-
CPY	0.32	-	**0.76**	-	0.21	-
BaA	-	0.21	**0.8**	-	-	-
IcdP	-	0.23	**0.75**	-	-	-
BghiP	0.28	-	**0.74**	-	0.37	-
BkF	0.32	-	**0.71**	-	0.37	0.23

BbF	0.22	0.28	**0.83**	-	0.27	-
BeP	0.27	0.21	**0.8**	-	0.32	-
BaP	-	-	**0.83**	-	0.34	-
CHRY	0.42	-	0.47	-	0.32	-
FLE	-	0.26	-	-	-	**0.73**
ANT (9,10)	-	-	-	0.2	0.25	0.2
FLO (9H)	-	-	0.24	0.44	-	0.42
BNT (2.2)	-	-	0.48	0.2	-	-
Glucose	-	0.51	-	-	0.22	-
Galactosan	-	0.31	-	0.34	0.2	0.23
Levoglucosan	0.27	0.41	-	0.31	-	-
Arabitol	-	**0.6**	-	0.3	-	-
Fructose	0.38	-	0.29	-	-	-

The first component rotated (PC1) explained 13% of the total variance in the dataset. PC1 exhibited high loadings for the metals Zn, Fe, Ba, Ca, Sn, and a minor loading for Sb, Cu, Mn, K. These metals could have their origins in road dust resuspension because of roadside particles contained in non – exhaust and exhaust car emissions. For instance (Pant and Harrison, 2013) have shown the emission of Zn and Ca from tire wear and Fe, Ba, Cu, Sb, and Sn from brake wear. Also, this component explained the variance of the n-alkane C_{21} and a variance proportion of the HMW PAH (DahA, CPY, BkF, BghiP, BbF) associated with vehicular emissions, together with Cu (Miguel and Pereira, 1989). Therefore, we call PC1 a component associated to road dust resuspension.

The second rotated component (PC2) explained 11% of the total variance. PC2 is a component associated with secondary aerosol formation and biomass burning. It was described by high loadings of the ions SO_4^{2-}, NH_4^+, methansulfonate, $C_2O_4^{2-}$, and NO_2^-, along with a fraction of EC and OC. Those ions also are observed in another region with sugarcane preharvest burning in Brazil (Allen et al., 2004), where the plume is enriched with Cl^-, NO_3^- and Na^+ in the fine fraction of aerosol particles, while the ions SO_4^{2-} and $C_2O_4^{2-}$ are formed in the atmosphere during transport process due to the oxidation of SO_2 and hydrocarbons. The important fraction of the variance of OC and especially EC explained by PC2 indicated the effect of an incomplete combustion process on this component, which together with the variance proportion explained by the Levoglucosan and K^+ indicated that the combustion process was associated with biomass burning. Also, PC2 is the one that best explained the variance of PAHs FLE and ANT, abundant in the chemical profile of sugarcane burning particles (Hall et al., 2012; Simoneit, 2002). Thus, PC2 seemed to be a combined effect of secondary aerosol formation and sugarcane burning.

The third rotated component (PC3) explained 11% of the variance and has high loadings for the PAH: BbF, BaP, BeP, BaA, CPY, IcdP, BghiP, BkF, and the n-alkane $C_{20}H_{42}$ typically emitted during incomplete combustion of vehicle fuels (Andrade et

al., 2012; Miguel and Pereira, 1989). A similar fraction of the variance of OC and EC was also explained with PC3, supporting the contribution of the combustion process. Thus, PC3 could be interpreted as a component derived from petroleum emissions by traffic.

The fourth rotated component (PC4) explained 10% of the variance and had high loadings for n-alkanes >C_{27}, K^+ and K. The n-alkanes >C_{25} are frequently associated with detritus and vegetable waxes. We explained the emission of the higher molecular weight n-alkanes to the biomass present in the region used by the agriculture industry and the abundance of nature present in the CRV. Therefore, we named PC4 a component associated with detritus vegetables.

The fifth rotated component (PC5) explained 9% of the variance, where C_{22} to C_{27} alkanes had high loadings. These fractions were associated with anthropogenic emissions (Kang et al., 2018). Thus, PC5 could be interpreted as a component derived from anthropogenic emissions. In addition, PC5 explained a variance proportion of some species associated with vehicular engine combustion, such as BghiP, BkF, BbF, characteristics of gasoline vehicles (Kuo et al., 2013) joint to EC and OC derivates from incomplete combustion. In summary, the components PC2, PC3 and PC5 describe the variance of EC, meaning the impact of incomplete combustion present in the region.

The sixth rotated component (PC6) explains 7% of the variance exhibiting high loadings for Mg^{2+}, Ca^{2+}, FLE, NO_3^+, and Cl^- and moderate for others such as $C_2O_4^{2-}$, Na^+, K^+. Particularly, the ions Cl^-, NO_3^+, K^+ increase during biomass burning (Ryu et al., 2004). In addition, PC6 strongly explained the variance of calcium as water soluble ions and a fraction of the trace metal, therefore the erosion of soil could be considered as an activity that explained PC6. After preharvest biomass burning and fires as a tool to prepare the land for the next crops the soil erosion can increase because of the reduction of vegetation. Therefore, compounds associated with soil erosion and derivates of biomass burning can simultaneously affect the soil erosion and the chemical composition of $PM_{2.5}$.

The PCA results showed there was no dominant component that explained the variance of chemical species contained in $PM_{2.5}$ in CRV. Instead, many components have roles equally important that are associated with road dust derived from traffic, the formation of secondary aerosol particles and biomass combustion, petroleum combustion associated with vehicular exhaust, and the presence of vegetative detritus and agriculture soil resuspended by wind erosion. Sugarcane burning was not identified as an individual component that can be explained because the open sugarcane burns happened continuously during the sampling, so they became a background source for this study that very likely was included in the secondary formation as another background source. However, the carbohydrates contained in $PM_{2.5}$ was linked to the characteristic species of secondary aerosol formation and vegetative detritus. Therefore the secondary pollutants could also originate from the burning of sugarcane in the CRV, similar to the results reported by (Vasconcellos et al., 2007) in Brazil.

4. Conclusions

$PM_{2.5}$ samples collected in the Cauca River Valley, Colombia, were analyzed to determine the main chemical components of fine aerosol particles and to qualitatively identify aerosol sources using its chemical composition and diagnostic ratios ~~and principal component analysis (PCA)~~. The main $PM_{2.5}$ components were organic material (52.7%), followed by ~~ammonium~~ sulfate (~~16.12~~ 12.7%) and elemental carbon (~~6.95~~ 7.1%). The contribution of ~~secondary~~ organic material and inorganic ions ~~salts~~ was found to be significant and likely related to biomass burning and agro-industrial activities agricultural practices and estimated secondary aerosol formation was estimation of. EC and PAHs concentrations confirm the presence of incomplete combustion process in CRV. Diagnostic ratios applied to organic compounds indicate that $PM_{2.5}$ was emitted locally and had contributions of pyrogenic and petrogenic sources. In addition, levoglucosan and mannosan levels showed that biomass burning was ubiquitous during the sampling period. Fluoranthene (FLE) was the most abundant PAH, ~~confrieming~~ confirming the strong influence of emissions derived from the abundant biomass present in CRV associated to the agricultural activities. ~~sugarcane burning~~. Five-ring and six-ring PAH associated with vehicular emissions were also abundant in $PM_{2.5}$. Our measurements point to agricultural activities ~~sugarcane PHB~~ as the main source of PAH~~s~~ in CRV. The comparison of $PM_{2.5}$ concentrations and mutagenic potentials suggest that year-long sugarcane PHB in CRV, which is also conducted on less than half of the harvested area (34% in 2018) and over limited plots sizes (~6 ha median), leads to lower atmospheric pollutant burdens and mutagenic potentials compared to those at locations where the harvesting period is shorter (*zafra*) thus with higher burning rates.

~~Several sources were identified through PCA, including road dust, secondary aerosol particles, and biomass combustion, vehicle exhaust, vegetative detritus and resuspended agricultural soil likely induced by pre-harvest burning. Not one of these sources was dominant nor explained the chemical species variance of measured $PM_{2.5}$. Sugarcane burning was not identified as an independent source, but it was found related to the secondary aerosol formation component on PCA~~. To reach a complete identification and apportionment of $PM_{2.5}$ sources in similar areas to CRV, where there is a wide diversity of agro-industrial and urban typical sources is required include data about organic tracers of biogenic, coal combustion and garbage burning and emissions, carbon This link between sugarcane burning emissions and secondary aerosol formation requires further investigation. We found that the effects of agriculture on CRV's air quality, particularly of sugarcane preharvest burning are non-trivial. Besides primary particles, this activity generates SOA precursors, induces soil resuspension and is closely tied to diesel emissions during harvesting.

Author contribution: RJ, GR-S, and NR conceived and managed the project. LM-F, ACV-B, GR-S, and RJ set the instruments up and performed the aerosol sampling. LM-F carried out the sample chemical analysis at TROPOS with the guidance and support of DvP, MvP, KW and HH. LM-F and ACV-B analyzed the measurement results, including PCA and other techniques with the support of DvP and RJ. LM-F, RJ, NR and ACV-B prepared the manuscript with substantial contributions from all the authors.

Competing interests: The authors declare that they have no conflict of interest.

Acknowledgments: The authors gratefully acknowledge the financial support from the Universidad Nacional de Colombia – Sede Palmira ([Impacto de la quema de caña de azúcar en la calidad del aire del Valle Geografico del Río Cauca] CACIQUE project Hermes # 37718) and Leibniz Institute for Tropospheric Research (TROPOS) for analytical support. This project was supported by EU granted the mobility project PAPILA. We thank Susanne Fuchs, Anke Roedger, Sylvia Haferkorn, and Kornelia Pielok for their technical assistance in the chemical analysis of samples. We acknowledge Pablo Gutierrez for his contributions in the processing of open sugarcane burning base data.

References

Abdurrahman, M. I., Chaki, S. and Saini, G.: Stubble burning: Effects on health & environment, regulations and management practices, Environ. Adv., 2(September), 100011, https://doi.org/10.1016/j.envadv.2020.100011, 2020.

Aerocivil: Estadísticas Operacionales, Operaciones aéreas Total. 2000-2019, 2019.

Agarwal, A., Satsangi, A., Lakhani, A. and Kumari, K. M.: Seasonal and spatial variability of secondary inorganic aerosols in PM2.5 at Agra: Source apportionment through receptor models, Chemosphere, 242, 125132, https://doi.org/10.1016/j.chemosphere.2019.125132, 2020.

Allen, A. G., Cardoso, A. A. and Da Rocha, G. O.: Influence of sugar cane burning on aerosol soluble ion composition in Southeastern Brazil, Atmos. Environ., 38(30), 5025–5038, https://doi.org/10.1016/j.atmosenv.2004.06.019, 2004.

Alvi, M. U., Kistler, M., Shahid, I., Alam, K., Chishtie, F., Mahmud, T. and Kasper-Giebl, A.: Composition and source apportionment of saccharides in aerosol particles from an agro-industrial zone in the Indo-Gangetic Plain, Environ. Sci. Pollut. Res. 2020 2712, 27(12), 14124–14137, https://doi.org/10.1007/S11356-020-07905-2, 2020.

Amador-Muñoz, O., Villalobos-Pietrini, R., Miranda, J. and Vera-Avila, L. E.: Organic compounds of PM2.5 in Mexico Valley: Spatial and temporal patterns, behavior and sources, Sci. Total Environ., 409(8), 1453–1465, https://doi.org/10.1016/j.scitotenv.2010.11.026, 2011.

Andrade, M. D. F., Miranda, R. M. De, Fornaro, A., Kerr, A., Oyama, B., Andre, P. A. De and Saldiva, P.: Vehicle emissions and PM2.5 mass concentrations in six Brazilian cities, , 79–88, https://doi.org/10.1007/s11869-010-0104-5, 2012.

de Andrade, S. J., Cristale, J., Silva, F. S., Julião Zocolo, G. and Marchi, M. R. R.: Contribution of sugar-cane harvesting

season to atmospheric contamination by polycyclic aromatic hydrocarbons (PAHs) in Araraquara city, Southeast Brazil, Atmos. Environ., 44(24), 2913–2919, https://doi.org/10.1016/j.atmosenv.2010.04.026, 2010.

Andreae, M. O.: Soot Carbon and Excess Fine Potassium : Long-Range Transport of Combustion-Derived Aerosols., 1983.

Aneja, V. P., Schlesinger, W. H. and Erisman, J. W.: Farming pollution, Nat. Geosci., 1(7), 409–411, https://doi.org/10.1038/ngeo236, 2008.

Aneja, V. P., Schlesinger, W. H. and Erisman, J. W.: Effects of agriculture upon the air quality and climate: Research, policy, and regulations, Environ. Sci. Technol., 43(12), 4234–4240, https://doi.org/10.1021/es8024403, 2009.

Asocaña: Aspectos Generales del Sector Agroindustrial de la Caña 2017 - 2018. Informe Anual., 2018.

Asocaña: Aspectos generales del sector agroindustial de la caña Informe anual 2018-2019., 2019.

Asocaña: Somos azucar y mucho más - Informe Anual 2019 - 2020., 2020.

De Assuncao, J. V., Pesquero, C. R., Nardocci, A. C., Francisco, A. P., Soares, N. S. and Ribeiro, H.: Airborne polycyclic aromatic hydrocarbons in a medium-sized city affected by preharvest sugarcane burning and inhalation risk for human health, J. Air Waste Manag. Assoc., 64(10), 1130–1139, https://doi.org/10.1080/10962247.2014.928242, 2014.

Begam, G. R., Vachaspati, C. V., Ahammed, Y. N., Kumar, K. R., Reddy, R. R., Sharma, S. K., Saxena, M. and Mandal, T. K.: Seasonal characteristics of water-soluble inorganic ions and carbonaceous aerosols in total suspended particulate matter at a rural semi-arid site, Kadapa (India), Environ. Sci. Pollut. Res., 24(2), 1719–1734, https://doi.org/10.1007/s11356-016-7917-1, 2016.

Bhattarai, H., Saikawa, E., Wan, X., Zhu, H., Ram, K., Gao, S., Kang, S., Zhang, Q., Zhang, Y., Wu, G., Wang, X., Kawamura, K., Fu, P. and Cong, Z.: Levoglucosan as a tracer of biomass burning: Recent progress and perspectives, Atmos. Res., 220(November 2018), 20–33, https://doi.org/10.1016/j.atmosres.2019.01.004, 2019.

Boman, J., Lindén, J., Thorsson, S., Holmer, B. and Eliasson, I.: A tentative study of urban and suburban fine particles (PM2.5) collected in Ouagadougou, Burkina Faso, X-Ray Spectrom., 38(4), 354–362, https://doi.org/10.1002/XRS.1173, 2009.

Cardozo-Valencia, A., Saa, G. R., Hernandez, A. J., Lopez, G. R. and Jimenez, R.: Distribución espaciotemporal y estimación de emisiones por quema precosecha de caña de azúcar en el Valle del Cauca, Conf. Proc. - Congr. Colomb. y Conf. Int. Calid. Aire y Salud Publica, CASAP 2019, https://doi.org/10.1109/CASAP.2019.8916696, 2019.

Casey, K. D., Bicudo, J. R., Schmidt, D. R., Singh, A., Gay, S. W., Gates, R. S., Jacobson, L. D. and Hoff, S. J.: Air quality and emissions from livestock and poultry production / waste management systems, in Animal Agriculture and the Environment, National Center for Manure & Animal Waste Management White Papers, pp. 1–40, , 2006.

Caumo, S., Bruns, R. E. and Vasconcellos, P. C.: Variation of the distribution of atmospheric n-alkanes emitted by different fuels' combustion, Atmosphere (Basel)., 11(6), 1–19, https://doi.org/10.3390/atmos11060643, 2020.

Cavalli, F., Viana, M., Yttri, K. E., Genberg, J. and Putaud, J.: Toward a standardised thermal-optical protocol for measuring atmospheric organic and elemental carbon : the EUSAAR protocol, , 79–89, 2010.

Chen, J., Li, C., Ristovski, Z., Milic, A., Gu, Y., Islam, M. S., Wang, S., Hao, J., Zhang, H., He, C., Guo, H., Fu, H., Miljevic,

B., Morawska, L., Thai, P., LAM, Y. F., Pereira, G., Ding, A., Huang, X. and Dumka, U. C.: A review of biomass burning: Emissions and impacts on air quality, health and climate in China, Sci. Total Environ., 579(November 2016), 1000–1034, https://doi.org/10.1016/j.scitotenv.2016.11.025, 2017.

Chow, J. C., Lowenthal, D. H., Chen, L. W. A., Wang, X. and Watson, J. G.: Mass reconstruction methods for PM2.5: a review, Air Qual. Atmos. Heal., 8(3), 243–263, https://doi.org/10.1007/s11869-015-0338-3, 2015.

Clegg, S. L. and Peter Brimblecombe, and A. S. W.: Thermodynamic Model of the System H+−NH4+−SO42-−NO3-−H2O at Tropospheric Temperatures, J. Phys. Chem. A, 102(12), 2137–2154, 1998.

Criollo, J. and Daza, N.: Evaluación de los niveles de concentración de metales en PM 10 producto de la quema de biomasa en el valle geográfico del rio Cauca, Universidad de la Salle, 2011.

Dabek-Zlotorzynska, E., Dann, T. F., Kalyani Martinelango, P., Celo, V., Brook, J. R., Mathieu, D., Ding, L. and Austin, C. C.: Canadian National Air Pollution Surveillance (NAPS) PM2.5 speciation program: Methodology and PM2.5 chemical composition for the years 2003-2008, Atmos. Environ., 45(3), 673–686, https://doi.org/10.1016/j.atmosenv.2010.10.024, 2011.

Dajuma, A., Ogunjobi, K. O., Vogel, H., Knippertz, P., Siluś, S., N'Datchoh, E. T., Yoboué, V. and Vogel, B.: Downward cloud venting of the central African biomass burning plume during the West Africa summer monsoon, Atmos. Chem. Phys., 20(9), 5373–5390, https://doi.org/10.5194/acp-20-5373-2020, 2020.

Dávalos, E.: La caña de azúcar: ¿una amarga externalidad? *, Desarro. Soc., 59, 117–164, 2007.

Durant, J. L., Busby, W. F., Lafleur, A. L., Penman, B. W. and Crespi, C. L.: Human cell mutagenicity of oxygenated, nitrated and unsubstituted polycyclic aromatic hydrocarbons associated with urban aerosols, Mutat. Res. - Genet. Toxicol., 371(3–4), 123–157, https://doi.org/10.1016/S0165-1218(96)90103-2, 1996.

El-Zanan, H. S., Lowenthal, D. H., Zielinska, B., Chow, J. C. and Kumar, N.: Determination of the organic aerosol mass to organic carbon ratio in IMPROVE samples, Chemosphere, 60(4), 485–496, https://doi.org/10.1016/j.chemosphere.2005.01.005, 2005.

Engling, G., Lee, J. J., Tsai, Y.-W., Lung, S.-C. C., Chou, C. C.-K. and Chan, C.-Y.: Size-Resolved Anhydrosugar Composition in Smoke Aerosol from Controlled Field Burning of Rice Straw, Aerosol Sci. Technol., 43(7), 662–672, https://doi.org/10.1080/02786820902825113, 2009.

FAO: FAOSTAT, 2020.

Fomba, K. ., Müller, K., Van Pinxteren, D. and Herrmann, H.: Aerosol size-resolved trace metal composition in remote northern tropical Atlantic marine environment: case study Cape Verde islands, Atmos. Chem. Phys., 13(9), 4801–4814, https://doi.org/10.5194/acp-13-4801-2013, 2013.

Fomba, K. W., van Pinxteren, D., Müller, K., Spindler, G. and Herrmann, H.: Assessment of trace metal levels in size-resolved particulate matter in the area of Leipzig, Atmos. Environ., 176, https://doi.org/10.1016/j.atmosenv.2017.12.024, 2018.

Franzin, B. T., Guizellini, F. C., de Babos, D. V., Hojo, O., Pastre, I. A., Marchi, M. R. R., Fertonani, F. L. and Oliveira, C.

M. R. R.: Characterization of atmospheric aerosol (PM10 and PM2.5) from a medium sized city in São Paulo state, Brazil, J. Environ. Sci. (China), 89, 238–251, https://doi.org/10.1016/j.jes.2019.09.014, 2020.

Friese, E. and Ebel, A.: Temperature Dependent Thermodynamic Model of the System H + - NH 4 + - Na + - SO 42 - - NO 3 - - Cl - - H 2 O., 2010.

Gonçalves, C., Figueiredo, B. R., Alves, C. A., Cardoso, A. A. and Vicente, A. M.: Size-segregated aerosol chemical composition from an agro-industrial region of São Paulo state, Brazil, Air Qual. Atmos. Heal. 2016 104, 10(4), 483–496, https://doi.org/10.1007/S11869-016-0441-0, 2016.

Gondwe, M.: Comparison of modeled versus measured MSA : nss SO = 4 ratios : A global analysis, , 18, 1–18, https://doi.org/10.1029/2003GB002144, 2004.

H M Malcolm and Dobson, S.: The calculation of an Environmental Assessment Level (EAL) for atmospheric PAHs using relative potencies., 1994.

Hall, D., Wu, C. Y., Hsu, Y. M., Stormer, J., Engling, G., Capeto, K., Wang, J., Brown, S., Li, H. W. and Yu, K. M.: PAHs, carbonyls, VOCs and PM 2.5 emission factors for pre-harvest burning of Florida sugarcane, Atmos. Environ., 55, 164–172, https://doi.org/10.1016/j.atmosenv.2012.03.034, 2012.

He, C., Miljevic, B., Crilley, L. R., Surawski, N. C., Bartsch, J., Salimi, F., Uhde, E., Schnelle-Kreis, J., Orasche, J., Ristovski, Z., Ayoko, G. A., Zimmermann, R. and Morawska, L.: Characterisation of the impact of open biomass burning on urban air quality in Brisbane, Australia, Environ. Int., 91(x), 230–242, https://doi.org/10.1016/j.envint.2016.02.030, 2016.

Hernández, J. D. R. and Mesa, Ó. J.: A simple conceptual model for the heat induced circulation over Northern South America and MESO-America, Atmosphere (Basel)., 11(11), 1–14, https://doi.org/10.3390/atmos11111235, 2020.

Hopke, P. K.: Review of receptor modeling methods for source apportionment, J. Air Waste Manage. Assoc., 66(3), 237–259, https://doi.org/10.1080/10962247.2016.1140693, 2016.

Ianniello, A., Spataro, F., Esposito, G., Allegrini, I., Hu, M. and Zhu, T.: and Physics Chemical characteristics of inorganic ammonium salts in PM 2 . 5 in the atmosphere of Beijing (China), , (October), https://doi.org/10.5194/acp-11-10803-2011, 2011.

IDEAM: 1er Inventario indicativo nacional de emisiones de contaminantes criterio & carbono negro 2010-2014, Bogotá D.C., 2018.

Iinuma, Y., Engling, G., Puxbaum, H. and Herrmann, H.: A highly resolved anion-exchange chromatographic method for determination of saccharidic tracers for biomass combustion and primary bio-particles in atmospheric aerosol, Atmos. Environ., 43(6), 1367–1371, https://doi.org/10.1016/J.ATMOSENV.2008.11.020, 2009.

Janta, R., Sekiguchi, K., Yamaguchi, R., Sopajaree, K., Pongpiachan, S. and Chetiyanukornkul, T.: Ambient PM2.5, polycyclic aromatic hydrocarbons and biomass burning tracer in Mae Sot District, western Thailand, Atmos. Pollut. Res., 11(1), 27–39, https://doi.org/10.1016/j.apr.2019.09.003, 2020.

Jenkins, B. M., Turn, S. Q. and Williams, R. B.: Atmospheric emissions from agricultural burning in California: Determination

of burn fractions, distribution factors, and crop-specific contributions, Agric. Ecosyst. Environ., 38(4), 313–330, https://doi.org/10.1016/0167-8809(92)90153-3, 1992.

Johnston, H. J., Mueller, W., Steinle, S., Vardoulakis, S., Tantrakarnapa, K., Loh, M. and Cherrie, J. W.: How Harmful Is Particulate Matter Emitted from Biomass Burning? A Thailand Perspective, Curr. Pollut. Reports, 5(4), 353–377, https://doi.org/10.1007/s40726-019-00125-4, 2019.

Jorquera, H. and Barraza, F.: Source apportionment of ambient PM2.5 in Santiago, Chile: 1999 and 2004 results, Sci. Total Environ., 435–436, 418–429, https://doi.org/10.1016/j.scitotenv.2012.07.049, 2012.

Jorquera, H. and Barraza, F.: Source apportionment of PM10 and PM2.5 in a desert region in northern Chile, Sci. Total Environ., 444, 327–335, https://doi.org/10.1016/j.scitotenv.2012.12.007, 2013.

Kang, M., Ren, L., Ren, H., Zhao, Y., Kawamura, K., Zhang, H., Wei, L., Sun, Y., Wang, Z. and Fu, P.: Primary biogenic and anthropogenic sources of organic aerosols in Beijing, China: Insights from saccharides and n-alkanes, Environ. Pollut., 243, 1579–1587, https://doi.org/10.1016/j.envpol.2018.09.118, 2018.

Karagulian, F., Belis, C. A., Francisco, C., Dora, C., Prüss-ustün, A. M., Bonjour, S., Adair-rohani, H. and Amann, M.: Contributions to cities ' ambient particulate matter (PM): A systematic review of local source contributions at global level, Atmos. Environ., 120, 475–483, https://doi.org/10.1016/j.atmosenv.2015.08.087, 2015.

Khedidji, S., Müller, K., Rabhi, L., Spindler, G., Fomba, K. W., Pinxteren, D. van, Yassaa, N. and Herrmann, H.: Chemical Characterization of Marine Aerosols in a South Mediterranean Coastal Area Located in Bou Ismaïl, Algeria, Aerosol Air Qual. Res., 20(January), https://doi.org/10.4209/aaqr.2019.09.0458, 2020.

Kundu, S. and Stone, E. A.: Composition and sources of fine particulate matter across urban and rural sites in the Midwestern United States, Environ. Sci. Process. Impacts, 16(6), 1360–1370, https://doi.org/10.1039/c3em00719g, 2014.

Kuo, C. Y., Chien, P. S., Kuo, W. C., Wei, C. T. and Rau, J. Y.: Comparison of polycyclic aromatic hydrocarbon emissions on gasoline- and diesel-dominated routes, Environ. Monit. Assess., 185(7), 5749–5761, https://doi.org/10.1007/s10661-012-2981-6, 2013.

Lara, L. L., Artaxo, P., Martinelli, L. A., Camargo, P. B., Victoria, R. L. and Ferraz, E. S. B.: Properties of aerosols from sugar-cane burning emissions in Southeastern Brazil, Atmos. Environ., 39(26), 4627–4637, https://doi.org/10.1016/j.atmosenv.2005.04.026, 2005.

Lee, S., Wang, Y. and Russell, A. G.: Assessment of secondary organic carbon in the southeastern United States: A review, J. Air Waste Manag. Assoc., 60(11), 1282–1292, https://doi.org/10.3155/1047-3289.60.11.1282, 2010.

Lee, T., Yu, X., Kreidenweis, S. M., Malm, W. C. and Collett, J. L.: Semi-continuous measurement of PM 2 . 5 ionic composition at several rural locations in the United States, , 42, 6655–6669, https://doi.org/10.1016/j.atmosenv.2008.04.023, 2008.

Li, F., Zhang, X. and Kondragunta, S.: Biomass burning in Africa: An investigation of fire radiative power missed by MODIS using the 375 m VIIRS active fire product, Remote Sens., 12(10), https://doi.org/10.3390/rs12101561, 2020.

Li, J., Song, Y., Mao, Y., Mao, Z., Wu, Y., Li, M., Huang, X., He, Q. and Hu, M.: Chemical characteristics and source apportionment of PM2.5 during the harvest season in eastern China's agricultural regions, Atmos. Environ., 92, 442–448, https://doi.org/10.1016/J.ATMOSENV.2014.04.058, 2014.

Li, X., Wang, L., Ji, D., Wen, T., Pan, Y., Sun, Y. and Wang, Y.: Characterization of the size-segregated water-soluble inorganic ions in the Jing-Jin-Ji urban agglomeration: Spatial/temporal variability, size distribution and sources, Atmos. Environ., 77, 250–259, https://doi.org/10.1016/j.atmosenv.2013.03.042, 2013.

Liang, C. S., Duan, F. K., He, K. Bin and Ma, Y. L.: Review on recent progress in observations, source identifications and countermeasures of PM2.5, Environ. Int., 86, 150–170, https://doi.org/10.1016/j.envint.2015.10.016, 2016.

Lin, L., Lee, M. L. and Eatough, D. J.: Review of recent advances in detection of organic markers in fine particulate matter and their use for source apportionment, J. Air Waste Manag. Assoc., 60(1), 3–25, https://doi.org/10.3155/1047-3289.60.1.3, 2010.

Lopez, M. and Howell, W.: Katabatic Winds in the equatorial Andes, J. Atmos. Sci., 24(1), 29–35, 1967.

Lyu, R., Shi, Z., Alam, M. S., Wu, X., Liu, D., Vu, T. V., Stark, C., Xu, R., Fu, P., Feng, Y. and Harrison, R. M.: Alkanes and aliphatic carbonyl compounds in wintertime PM2.5 in Beijing, China, Atmos. Environ., 202(November 2018), 244–255, https://doi.org/10.1016/j.atmosenv.2019.01.023, 2019.

MADS: Res. No 2254, Ministerio de Ambiente y Desarrollo Sostenible, Colombia., 2017.

Majra, J. P.: Air Quality in Rural Areas, in Chemistry, Emission Control, Radioactive Pollution and Indoor Air Quality, https://doi.org/10.5772/16890, , 2011.

Mancilla, Y., Mendoza, A., Fraser, M. P. and Herckes, P.: Organic composition and source apportionment of fine aerosol at Monterrey, Mexico, based on organic markers, Atmos. Chem. Phys., 16(2), 953–970, https://doi.org/10.5194/acp-16-953-2016, 2016.

Marzi, R., Torkelson, B. E. and Olson, R. K.: A revised carbon preference index, Org. Geochem., 20(8), 1303–1306, https://doi.org/10.1016/0146-6380(93)90016-5, 1993.

Mesa S., Ó. J. and Rojo H., J. D.: On the general circulation of the atmosphere around Colombia, Rev. la Acad. Colomb. Ciencias Exactas, Fis. y Nat., 44(172), 857–875, https://doi.org/10.18257/RACCEFYN.899, 2020.

Miguel, A. H. and Pereira, P. A. P.: Benzo(k)fluoranthene, benzo(ghi)perylene, and indeno(1, 2, 3-cd)pyrene: New tracers of automotive emissions in receptor modeling, Aerosol Sci. Technol., 10(2), 292–295, https://doi.org/10.1080/02786828908959265, 1989.

Min.Agricultura: Cadenas cárnicas bovina - bufalina, Bogotá D.C., 2018.

Min.Agricultura: Cadena Carnica Porcina, Bogotá D.C., 2019.

Min.Agricultura: Cadena Avícola, segundo trimestre 2020, Bogotá D.C., 2020.

Mkoma, S. L., Kawamura, K. and Fu, P. Q.: Contributions of biomass/biofuel burning to organic aerosols and particulate matter in Tanzania, East Africa, based on analyses of ionic species, organic and elemental carbon, levoglucosan and mannosan,

Atmos. Chem. Phys., 13(20), 10325–10338, https://doi.org/10.5194/acp-13-10325-2013, 2013.
Mugica-Alvarez, V., Santiago-de la Rosa, N., Figueroa-Lara, J., Flores-Rodríguez, J., Torres-Rodríguez, M. and Magaña-Reyes, M.: Emissions of PAHs derived from sugarcane burning and processing in Chiapas and Morelos México, Sci. Total Environ., 527–528, 474–482, https://doi.org/10.1016/j.scitotenv.2015.04.089, 2015.
Mugica-Álvarez, V., Ramos-Guízar, S., Rosa, N. S. la, Torres-Rodríguez, M. and Noreña-Franco, L.: Black Carbon and Particulate Organic Toxics Emitted by Sugarcane Burning in Veracruz, México, Int. J. Environ. Sci. Dev., 7(4), 290–294, https://doi.org/10.7763/ijesd.2016.v7.786, 2016.
Mugica-Álvarez, V., Hernández-Rosas, F., Magaña-Reyes, M., Herrera-Murillo, J., Santiago-De La Rosa, N., Gutiérrez-Arzaluz, M., de Jesús Figueroa-Lara, J. and González-Cardoso, G.: Sugarcane burning emissions: Characterization and emission factors, Atmos. Environ., 193, 262–272, https://doi.org/10.1016/j.atmosenv.2018.09.013, 2018.
Murillo, J. H., Roman, S. R., Felix, J., Marin, R., Ramos, A. C., Jimenez, S. B., Gonzalez, B. C. and Baumgardner, D. G.: Chemical characterization and source apportionment of PM10 and PM2.5 in the metropolitan area of Costa Rica, Central America Jorge, Atmos. Pollut. Res., 4(2), 181–190, https://doi.org/10.5094/APR.2013.018, 2013.
Neusüss, C., Pelzing, M., Plewka, A. and Herrmann, H.: A new analytical approach for size-resolved speciation of organic compounds in atmospheric aerosol particles: Methods and first results, J. Geophys. Res. Atmos., 105(D4), 4513–4527, https://doi.org/10.1029/1999JD901038, 2000.
Nisbet, I. C. T. and LaGoy, P. K.: Toxic equivalency factors (TEFs) for polycyclic aromatic hydrocarbons (PAHs), Regul. Toxicol. Pharmacol., 16(3), 290–300, https://doi.org/10.1016/0273-2300(92)90009-X, 1992.
Oros, D. R., Abas, M. R. bin, Omar, N. Y. M. J., Rahman, N. A. and Simoneit, B. R. T.: Identification and emission factors of molecular tracers in organic aerosols from biomass burning: Part 3. Grasses, Appl. Geochemistry, 21(6), 919–940, https://doi.org/10.1016/j.apgeochem.2006.01.008, 2006.
Ortiz, E. Y., Jimenez, R., Fochesatto, G. J. and Morales-Rincon, L. A.: Caracterización de la turbulencia atmosférica en una gran zona verde de una megaciudad andina tropical, Rev. la Acad. Colomb. Ciencias Exactas, Físicas y Nat., 43(166), 133, https://doi.org/10.18257/raccefyn.697, 2019.
Pan, X., Ichoku, C., Chin, M., Bian, H., Darmenov, A., Colarco, P., Ellison, L., Kucsera, T., Da Silva, A., Wang, J., Oda, T. and Cui, G.: Six global biomass burning emission datasets: Intercomparison and application in one global aerosol model, Atmos. Chem. Phys., 20(2), 969–994, https://doi.org/10.5194/acp-20-969-2020, 2020.
Pant, P. and Harrison, R. M.: Estimation of the contribution of road traffic emissions to particulate matter concentrations from field measurements: A review, Atmos. Environ., 77, 78–97, https://doi.org/10.1016/j.atmosenv.2013.04.028, 2013.
Pereira, G. M., Teinilä, K., Custódio, D., Gomes Santos, A., Xian, H., Hillamo, R., Alves, C. A., Bittencourt de Andrade, J., Olímpio da Rocha, G., Kumar, P., Balasubramanian, R., Andrade, M. de F. and de Castro Vasconcellos, P.: Particulate pollutants in the Brazilian city of São Paulo: 1-year investigation for the chemical composition and source apportionment, Atmos. Chem. Phys., 17(19), 11943–11969, https://doi.org/10.5194/acp-17-11943-2017, 2017.

Pereira, G. M., Oraggio, B., Teinilä, K., Custódio, D., Huang, X., Hillamo, R., Alves, C. A., Balasubramanian, R., Rojas, N. Y. and Sanchez-Ccoyllo, O.: A comparative chemical study of PM 10 in three Latin American cities : Lima, Medellín, ans São Paulo, Air Qual. Atmos. Heal., 12, 1141–1152, https://doi.org/10.1007/s11869-019-00735-3, 2019.

Pio, C., Cerqueira, M., Harrison, R. M., Nunes, T., Mirante, F., Alves, C., Oliveira, C., Sanchez de la Campa, A., Artíñano, B. and Matos, M.: OC/EC ratio observations in Europe: Re-thinking the approach for apportionment between primary and secondary organic carbon, Atmos. Environ., 45(34), 6121–6132, https://doi.org/10.1016/j.atmosenv.2011.08.045, 2011.

Plaza, J., Artíñano, B., Salvador, P., Gómez-Moreno, F. J., Pujadas, M. and Pio, C. A.: Short-term secondary organic carbon estimations with a modified OC/EC primary ratio method at a suburban site in Madrid (Spain), Atmos. Environ., 45(15), 2496–2506, https://doi.org/10.1016/j.atmosenv.2011.02.037, 2011.

Pongpiachan, S., Hattayanone, M. and Cao, J.: Effect of agricultural waste burning season on PM2.5-bound polycyclic aromatic hydrocarbon (PAH) levels in Northern Thailand, Atmos. Pollut. Res., 8(6), 1069–1080, https://doi.org/10.1016/j.apr.2017.04.009, 2017.

Pye, H. O. T., Nenes, A., Alexander, B., Ault, A. P., Barth, M. C., Clegg, S. L., Collett, J. L., Fahey, K. M., Hennigan, C. J., Herrmann, H., Kanakidou, M., Kelly, J. T., Ku, I. T., Faye McNeill, V., Riemer, N., Schaefer, T., Shi, G., Tilgner, A., Walker, J. T., Wang, T., Weber, R., Xing, J., Zaveri, R. A. and Zuend, A.: The acidity of atmospheric particles and clouds., 2020.

Ramírez, O., Sánchez de la Campa, A. M., Amato, F., Catacolí, R. A., Rojas, N. Y. and de la Rosa, J.: Chemical composition and source apportionment of PM10 at an urban background site in a high–altitude Latin American megacity (Bogota, Colombia), Environ. Pollut., 233, 142–155, https://doi.org/10.1016/j.envpol.2017.10.045, 2018.

Ravindra, K., Sokhi, R. and Van Grieken, R.: Atmospheric polycyclic aromatic hydrocarbons: Source attribution, emission factors and regulation, Atmos. Environ., 42(13), 2895–2921, https://doi.org/10.1016/j.atmosenv.2007.12.010, 2008.

Romero, D., Sarmiento, H. and Pachón, J. E.: Estimación de hidrocarburos aromáticos policíclicos y metales pesados asociados con la quema de caña de azúcar en el valle geográfico del río Cauca , Colombia, Rev. Épsilon, 21(2013), 57–82, 2013.

Ryu, S. Y., Kim, J. E., Zhuanshi, H., Kim, Y. J. and Kang, G. U.: Chemical composition of post-harvest biomass burning aerosols in gwangju, Korea, J. Air Waste Manag. Assoc., 54(9), 1124–1137, https://doi.org/10.1080/10473289.2004.10471018, 2004.

Dos Santos, C. Y. M., Azevedo, D. de A. and De Aquino Neto, F. R.: Selected organic compounds from biomass burning found in the atmospheric particulate matter over sugarcane plantation areas, Atmos. Environ., 36(18), 3009–3019, https://doi.org/10.1016/S1352-2310(02)00249-2, 2002.

Schauer, J. J.: Sources contributions to atmospheric organic compound concentrations: Emissions measurments and model predictions, California Institute Technology, 1998.

SDA: Plan decenal de descontaminación del aire de Bogotá, Bogotá D.C., 2010.

Seinfeld, J. H. and Pandis, S. N.: Atmospheric From Air Pollution to Climate Change., 2006.

SICOM: Boletín estadístico, Boletín Estad. EDS automotriz y Fluv., 2018.

Simoneit, B. R. T.: Biomass burning - A review of organic tracers for smoke from incomplete combustion, Appl. Geochemistry, 17(3), 129–162, https://doi.org/10.1016/S0883-2927(01)00061-0, 2002.

Snider, G., Weagle, C. L., Murdymootoo, K. K., Ring, A., Ritchie, Y., Stone, E., Walsh, A., Akoshile, C., Anh, N. X., Balasubramanian, R., Brook, J., Qonitan, F. D., Dong, J., Griffith, D., He, K., Holben, B. N., Kahn, R., Lagrosas, N., Lestari, P., Ma, Z., Misra, A., Norford, L. K., Quel, E. J., Salam, A., Schichtel, B., Segev, L., Tripathi, S., Wang, C., Yu, C., Zhang, Q., Zhang, Y., Brauer, M., Cohen, A., Gibson, M. D., Liu, Y., Martins, J. V., Rudich, Y. and Martin, R. V.: Variation in global chemical composition of PM2.5: emerging results from SPARTAN, Atmos. Chem. Phys., 16(15), 9629–9653, https://doi.org/10.5194/acp-16-9629-2016, 2016.

Sorooshian, A., Crosbie, E., Maudlin, L. C., Youn, J., Wang, Z., Shingler, T., Ortega, A. M., Hersey, S. and Woods, R. K.: Surface and airborne measurements of organosulfur and methanesulfonate over the western United States and coastal areas, J. Geophys. Res. Atmos., 8535–8548, https://doi.org/10.1002/2015JD023822.Received, 2015.

Souza, D. Z., Vasconcellos, P. C., Lee, H., Aurela, M., Saarnio, K., Teinilä, K. and Hillamo, R.: Composition of PM2.5 and PM10 collected at Urban Sites in Brazil, Aerosol Air Qual. Res., 14(1), 168–176, https://doi.org/10.4209/aaqr.2013.03.0071, 2014.

Sutton, M. A., Billen, G., Bleeker, A., Erisman, J. W., Grennfelt, P., Grinsven, H. Van, Grizzetti, B., Howard, C. M. and Leip, A.: Technical summary Part I Nitrogen in Europe : the present position, , (December 2015), 2011.

Szabó, J., Szabó Nagy, A. and Erdős, J.: Ambient concentrations of PM10, PM10-bound polycyclic aromatic hydrocarbons and heavy metals in an urban site of Győr, Hungary, Air Qual. Atmos. Heal., 8(2), 229–241, https://doi.org/10.1007/s11869-015-0318-7, 2015.

Tang, M., Guo, L., Bai, Y., Huang, R., Wu, Z. and Wang, Z.: Impacts of methanesulfonate on the cloud condensation nucleation activity of sea salt aerosol, Atmos. Environ., 201(October 2018), 13–17, https://doi.org/10.1016/j.atmosenv.2018.12.034, 2019.

Tobiszewski, M. and Namieśnik, J.: PAH diagnostic ratios for the identification of pollution emission sources, Environ. Pollut., 162(November 2018), 110–119, https://doi.org/10.1016/j.envpol.2011.10.025, 2012.

Turpin, B. J. and Lim, H.: Species Contributions to PM2 . 5 Mass Concentrations : Revisiting Common Assumptions for Estimating Organic Mass, Aerosol Sci. Technol., 35:1(September 2014), 37–41, https://doi.org/http://dx.doi.org/10.1080/02786820119445, 2001.

Urban, R. C., Lima-Souza, M., Caetano-Silva, L., Queiroz, M. E. C., Nogueira, R. F. P., Allen, A. G., Cardoso, A. A., Held, G. and Campos, M. L. A. M.: Use of levoglucosan, potassium, and water-soluble organic carbon to characterize the origins of biomass-burning aerosols, Atmos. Environ., 61, 562–569, https://doi.org/10.1016/j.atmosenv.2012.07.082, 2012.

Urban, R. C., Alves, C. A., Allen, A. G., Cardoso, A. A., Queiroz, M. E. C. and Campos, M. L. A. M.: Sugar markers in aerosol particles from an agro-industrial region in Brazil, Atmos. Environ., 90(2014), 106–112, https://doi.org/10.1016/j.atmosenv.2014.03.034, 2014.

Urban, R. C., Alves, C. A., Allen, A. G., Cardoso, A. A. and Campos, M. L. A. M.: Organic aerosols in a Brazilian agro-industrial area: Speciation and impact of biomass burning, Atmos. Res., 169, 271–279, https://doi.org/10.1016/j.atmosres.2015.10.008, 2016.

Vargas, F. A., Rojas, N. Y., Pachon, J. E. and Russell, A. G.: PM10 characterization and source apportionment at two residential areas in Bogota, Atmos. Pollut. Res., 3(1), 72–80, https://doi.org/10.5094/APR.2012.006, 2012.

Vasconcellos, P. C., Balasubramanian, R., Bruns, R. E., Sanchez-Ccoyllo, O., Andrade, M. F. and Flues, M.: Water-soluble ions and trace metals in airborne particles over urban areas of the state of São Paulo, Brazil: Influences of local sources and long range transport, Water. Air. Soil Pollut., 186(1–4), 63–73, https://doi.org/10.1007/s11270-007-9465-2, 2007.

Vasconcellos, P. C., Souza, D. Z., Ávila, S. G., Araújo, M. P., Naoto, E., Nascimento, K. H., Cavalcante, F. S., Dos, M., Smichowski, P. and Behrentz, E.: Comparative study of the atmospheric chemical composition of three South American cities, Atmos. Environ., 45(32), 5770–5777, https://doi.org/10.1016/j.atmosenv.2011.07.018, 2011.

Victoria, J., Amaya, A., Rangel, H., Viveros, C., Cassalett, C., Carbonell, J., Quintero, R., Cruz, R., Isaacs, C., Larrahondo, J., Moreno, C., Palma, A., Posada, C., Villegas, F. and Gómez, L.: Características agronómicas y de productividad de la variedad Cenicaña Colombiana (CC) 85-92, Cali., 2002.

Villalobos, A. M., Barraza, F., Jorquera, H. and Schauer, J. J.: Chemical speciation and source apportionment of fine particulate matter in Santiago, Chile, 2013, Sci. Total Environ., 512–513, 133–142, https://doi.org/10.1016/j.scitotenv.2015.01.006, 2015.

Wadinga Fomba, K., Deabji, N., El Islam Barcha, S., Ouchen, I., Mehdi Elbaramoussi, E., Cherkaoui El Moursli, R., Harnafi, M., El Hajjaji, S., Mellouki, A. and Herrmann, H.: Application of TXRF in monitoring trace metals in particulate matter and cloud water, Atmos. Meas. Tech., 13(9), 4773–4790, https://doi.org/10.5194/amt-13-4773-2020, 2020.

Wagner, R., Jähn, M. and Schepanski, K.: Wildfires as a source of airborne mineral dust - Revisiting a conceptual model using large-eddy simulation (LES), Atmos. Chem. Phys., 18(16), 11863–11884, https://doi.org/10.5194/acp-18-11863-2018, 2018.

Wang, L., Xin, J., Li, X. and Wang, Y.: The variability of biomass burning and its influence on regional aerosol properties during the wheat harvest season in North China, Atmos. Res., 157, 153–163, https://doi.org/10.1016/j.atmosres.2015.01.009, 2015.

Wang, Y., Yang, F., Li, X., Tian, M. and Hopke, P. K.: On the source contribution to Beijing PM2.5 concentrations, , 134, 84–95, https://doi.org/10.1016/j.atmosenv.2016.03.047, 2016.

Van Wees, D. and Van Der Werf, G. R.: Modelling biomass burning emissions and the effect of spatial resolution: A case study for Africa based on the Global Fire Emissions Database (GFED), Geosci. Model Dev., 12(11), 4681–4703, https://doi.org/10.5194/gmd-12-4681-2019, 2019.

WHO Regional Office for Europe: Air quality guidelines for Europe, pp. 457–465, World Health Organization, Copenhagen, Denmark, https://doi.org/10.1525/9780520948068-070, , 2020.

World Health Organization: Review of evidence on health aspects of air pollution - REVIHAAP Project., 2013.

World Health Organization: WHO global air quality guidelines: particulate matter (PM2.5 and PM10), ozone, nitrogen dioxide,

sulfur dioxide and carbon monoxide, World Health Organization., 2021.
Wu, C. and Zhen Yu, J.: Evaluation of linear regression techniques for atmospheric applications: The importance of appropriate weighting, Atmos. Meas. Tech., 11(2), 1233–1250, https://doi.org/10.5194/amt-11-1233-2018, 2018.
Yadav, I. C. and Devi, N. L.: Biomass burning, regional air quality, and climate change, Encycl. Environ. Heal., (April), 386–391, https://doi.org/10.1016/B978-0-12-409548-9.11022-X, 2019.
Yadav, S., Tandon, A. and Attri, A. K.: Monthly and seasonal variations in aerosol associated n-alkane profiles in relation to meteorological parameters in New Delhi, India, Aerosol Air Qual. Res., 13(1), 287–300, https://doi.org/10.4209/aaqr.2012.01.0004, 2013.
Yan, J., Wang, L., Fu, P. P. and Yu, H.: Photomutagenicity of 16 polycyclic aromatic hydrocarbons from the US EPA priority pollutant list, Mutat. Res. - Genet. Toxicol. Environ. Mutagen., 557(1), 99–108, https://doi.org/10.1016/j.mrgentox.2003.10.004, 2004.
Yunker, M. B., Macdonald, R. W., Vingarzan, R., Mitchell, H., Goyette, D. and Sylvestre, S.: PAHs in the Fraser River basin: a critical appraisal of PAH ratios as indicators of PAH source and composition, Org. Geochem., 33, 489–515, 2002.